SOFIA UNIVERSITY "ST. KLIMENT OHRIDSKI"

FACULTY OF PHYSICS

DEPARTMENT OF ATOMIC PHYSICS

# Abstract

of a dissertation for awarding the educational and scientific degree "Doctor of Philosophy"

on topic

# Methods for dosimetric assessment, optimization and control of radiotherapy plans

Dimitar Rosenov Penev

Academic supervisor: Dobromir S. Pressyanov, Ph.D., D.Sc., Professor

Scientific consultant: Pavel Stavrev, Ph.D

Sofia

2024

# *Table of contents*

# 1. Introduction

The fight against cancer is a growing challenge of our time. The statistics for 2020 are 36,451 new cases, with 19,460 deaths (53.4%). Leading in frequency are prostate cancer (13.7% of those diagnosed), colorectal carcinoma (12.8%), lung cancer (11.8%) and breast cancer (11.1%) [ **1** ]. The high mortality rate is a consequence of the undiagnosed or untimely diagnosis of cancer, and/or the untimely treatment. The treatment, in turn, includes various methods, which depending on the disease can be combined with each other - surgery (removal of part of the tumor or the entire tumor), radiation therapy (external and/or brachytherapy), chemotherapy and immunotherapy. Although more and more hospitals and radiation treatment centers have been opened in Bulgaria over the years, undiagnosed and untreated patients have a low survival rate, varying depending on the histology and stage of the disease. Radiation therapy, for its part, has developed extremely rapidly in the last two decades, following the advent of modern linear accelerators, which are used for treatment techniques such as - intensity modulated radiation therapy ( IMRT) , volumetric modulated arc therapy ( VMAT) [ **2, 3** ]. In the last few years, proton therapy has gained momentum as a more sparing method for the critical organs surrounding the irradiated tumor mass. This is due to the "Briag peak" and the ability of protons to release their energy "abruptly" in depth [ **4** ] - that is, we have a low output dose. They are particularly useful as a method of radiotherapy for childhood oncological diseases [ **5** ].

Radiation therapy is one of the main methods in the treatment of oncological and some non-oncological diseases using the ability of ionizing particles to release their energy in the patient.

The types of radiotherapy are divided into:

- External beam radiation therapy – the most common type of radiation therapy. The source of ionizing radiation is located outside the patient (per cutem – through the skin). Electron and/or photon linear accelerators, telegamatherapy unit (60 Co source) , surface/deep X-ray therapy unit, proton therapy unit are used.
- Brachytherapy - treatment involves placing a radioactive source in the natural human cavities near the tumor (intracavitary), interstitial - a source temporarily or permanently introduced into the tumor, contact - the source is placed on the surface of the skin and

metabolic brachytherapy - the radionuclide is injected into the circulatory system and accumulates in the tumor.

The current dissertation focuses on external beam radiation therapy with photon.

### 1.1. Objectives of the dissertation

The objectives of the dissertation work are:

- To track the progress of radiobiological models used to assess the tumor control probability and normal tissue complication probability. To consider the mechanisms of cell damage and their incorporation into the models themselves.
- To investigate the application of radiobiological models to assess the influence of hypoxia in hypofractionated radiation therapy.
- To investigate the influence of different intervals between irradiations on the tumor control probability.
- To investigate the impact of the uncertainty of the delivered dose in the tumor on the tumor control probability.

## 2. Dosimetry and dosimetric methods and tools in radiation therapy. Quality assurance

Dosimetry in radiation therapy and quality assurance of dosimetric equipment are part of the tasks of the medical physicist. There are a number of documents [ **6** , **7** , **8** , **9** , **10** ] that serve the medical physicist in conducting the various tests that verify the correctness of the equipment, as well as procedures for its calibration. Since radiation therapy is a complex process and is a set of different stages that it goes through, errors can occur in each of these stages, which are: scanning, immobilization, contouring of tumor volume and critical organs, treatment planning, execution of

the treatment plan, reproducibility of irradiation (when fractionating the therapy). Precisely to limit potential errors, different operating protocols are used, which may be hospital, national or international. Separately, it is necessary to ensure the quality of the dosimetric equipment through regular tests, the tolerances and frequency of which are listed in Regulation №2 of February 5, 2018 [ **11** ].

The need for quality assurance aims to achieve high tumor control and at the same time a low normal tissue complication probability - that is, to reduce the irradiation of critical organs to the minimum possible without compromising the treatment and achieving the desired therapeutic effect.

Part of the present dissertation is to assess how the uncertainties affect in the delivered dose on the tumor control probability. Although a theoretical study, it serves to illustrate how this uncertainty affects the outcome of radiotherapy and is discussed in **Chapter 6** . In theory, it can also be applied in practice, since radiobiological models serving to optimize (solve the "inverse" task) the dosimetric plan and its evaluation are integrated into the planning systems (TPS) of leading manufacturers such as Varian (Eclipse TPS), Electa (Monaco TPS), etc. Also, new and improved TCP/NTCP models are being devised by medical physicists working in practice and engaged in scientific work.

Information on the uncertainty of dosimetric measurements with an ionization chamber, which is routinely used in dosimetry of high-energy photon beams, is available [ **6 , 1 2** ] and justifies the conduct of such a study using TCP models, which are discussed in this dissertation. The ionization chambers used in the absolute dosimetry of high-energy photon beams have a volume between $0.1cm^3$ and $1cm^3$ [ **2** ] . This volume is a compromise and balance between sensitivity, which increases with increasing volume, and the ability to measure point dose. They must be "open" chambers so that they can quickly reach equilibrium with the environment (temperature and atmospheric pressure). The chamber walls are made of graphite, which has better reading stability than chambers with polymethyl methacrylate ( PMMA) walls .

## 3. Basic concepts and connections

In the presented dissertation, basic concepts related to the processes taking place in the tumor and tumor dynamics are considered, and subsequently various radiobiological models are used to evaluate the outcome of radiation therapy.

It is believed that the structure of DNA (deoxyribonucleic acid), which is a double-stranded helix made up of monosaccharides and phosphate groups connected to each other by ester bonds [ **13** ], is the main target when exposed to ionizing radiation [ **14** , **15** , **16** ]. Since this structure is the carrier of hereditary information and it is the basis of the ability of cells to transmit their genetic information through the process of replication, its damage can lead to cell death or the occurrence of mutations. Depending on the number and location of the break in the DNA structure, as a consequence of the passing ionizing particles, we have a single- or double-stranded break. A single-strand break is repairable [ **17** , **18** ] and the cell is likely to persist. In individual cases, it may not fully restore its functions and mutate. A double-strand break most likely leads to cell death. The two tears should be in close proximity. Then the cell has no mechanism to restore its normal functions and ceases to exist [ **19** , **20** ]. If the two breaks of the two chains are far enough apart, the cell has a mechanism to restore its functions [ **21** , **22** ].

Disruption of the DNA structure can occur in two ways. The first mechanism is the direct passage of the ionizing particle through the DNA strand and thus death/damage is directly induced. The second mechanism is indirect - in it, the ionizing particles creates reactive oxygen species. Examples are: superoxide anion ( $O_2^-$ ), hydrogen peroxide ($H_2O_2$ ), hydroxyl radical (HO•) , hydroxyl ion ($OH^-$ ), hydroperoxide radical, which are chemically highly reactive and attack adjacent biologically important molecules, causing chemical reactions in them and thus damage them [ **23** , **24** ].

In 1956, Puck et al. [ **25** ] published the first cell survival curve ( survival curve ≡ SC) of mammalian cells. This marked the beginning of modern radiation therapy. Three years later, Hewitt et al. [ **26** ] published a similar study on mammalian cells analyzed in vivo. Surviving fraction (SF) of cells represents the relative fraction of surviving cells $N_{surv}$ , after irradiation of a cell colony, with an initial number of cells $N_0$ , to dose $D$. The cell survival curve is the function

$S = SF(D)$ and shows the dependence between the survival fraction and the absorbed dose . This relationship is shown graphically, with survival fraction presented on the ordinate in a logarithmic scale and dose on the abscissa in a linear scale. For radiations with low linear energy transfer ( LET), the curve initially slopes, then follows a region with a shoulder, after which the curve, above a threshold high dose, straightens. For high- LET radiations , the curves are almost exponential, and on the log-linear scale they are represented by an almost straight line. The first models cannot completely fit the cell survival curves, and more precisely the part above a given threshold high dose. We will review basic models that underpin target theory and attempt to explain the mechanisms of cell killing.

Models that describe the cell 's response to ionizing radiation are: Single Hit Model , Multi Hit Model , Single hit - many targets " (Single Hit - Multi Target Model) , Linear-Quadratic Model , Linear-Quadratic-Linear Model. Since it is considered that the main target in the cell is DNA, Douglas Lea [ **27** ] gave the beginning of the so-called target theory, with one of the first models that succeeded in describing radiation-induced cell death, called the Single hit model.

We will focus on the linear-quadratic model as it is the most widely used and has been shown to describe radiation-induced cell death well. It is used in all the calculations in this dissertation.

In 1972 [ **28** ] and 1973 [ **29** ] respectively based on different considerations and using as a basis the research carried out by Lea et al. [ **27** , **30** ], two scientific groups introduced the linear-quadratic model. According to this model, cell killing occurs when at least two "fatal" hits occur, and these hits can be caused by one particle hitting both DNA strands at the same time, or by two particles each hitting one of the DNA strands. Since these two hitting modes are independent, the cell survival probability is given by:

$$p_s = p_1 p_2 \quad (1)$$

where $p_1$ is the probability of avoiding a "fatal" hit caused by one particle, and $p_2$ is the probability of avoiding a "fatal" hit caused by two particles.

$$p_s = e^{-\alpha D - \beta D^2} \quad (2)$$

where $\alpha$ and $\beta$ are parameters determining radiosensitivity and represent the probability of cell death upon the passage of one ( $\alpha$ ) and two ( $\beta$ ) particles.

Kellerer et al. [ **28** ] derive the linear-quadratic mechanism of cell damage based on microdosimetric considerations (influence of linear energy transfer ( LET ) and the relative biological effectiveness ( RBE ) to the processes occurring in the cell ) , while Chadwick et al. [ **29** ] derived equation ( **2** ) based on the molecular theory and the biological processes in the cell.

The main biological factors influencing radiation therapy will be reviewed sequentially. They are better known as the 5 "R's" in radiobiology – radiosensitivity, repopulation, reoxygenation, redistribution, repair, and play a key role in the fractionation of radiotherapy and its effectiveness.

- **Radiosensitivity:**

Cells in the body can have different radiosensitivity to different types of ionizing radiation. It depends on factors such as the type and energy of the radiation. With equal energy transferred to the living organism ( $D = d\bar{E} / dm$ , [J/kg]) , radiations with different linear energy transfer (LET) cause different effects. Based on the rate at which energy is deposited in cells, different radiations are with low linear energy transfer (such as photons and electrons) and with high linear energy transfer such as protons, neutrons, alpha particles, etc. [ **31** ]. The main application at the moment is radiation with low LET , but in recent years, therapy with protons, which have high LET and thanks to their characteristic to give off their energy sharply at the end of their pathway (Bragg peak). At the beginning of their pathway in the patient, when passing through healthy tissues, the protons have a low LET and when they reach the tumor they give all their energy for a very short time, the Bragg peak can be "tuned" by adjusting the energy of the beam , thus the depth to which the energy will be delivered is also regulated.

In order to be able to compare the effects of different types of radiation, the concept of relative biological effectiveness is introduced (RBE) or the ratio of the absorbed dose of a given radiation to the absorbed dose of the reference radiation, necessary to obtain an identical biological effect . LET depends on the mass (charge) and velocity of the particle. Heavier and slower particles (alpha particles, neutrons, heavy nuclei) have a greater LET. The maximum relative biological effectiveness of radiation is observed at LET~100keV/μm [ **32** ]. At this LET value, the distance

between ionization events is exactly equal to the diameter of the DNA double helix. Typical LET values for the various ionizing particles are: for X-rays, γ and $e^-$ → 0.2-0.5 keV/ μm ; for protons → 0.5-5 keV/ μm; for neutrons and alpha particles → ~100keV/μm. Higher LET values can induce denser ionizations, but these additional ionizations do not lead to additional double-strand breaks, so even after the threshold value of 100keV/μm, with increasing LET → RBE decreases.

- **Repopulation:**

Repopulation is the property of tumor cells to intensively proliferate after irradiation with ionizing radiation. This gives them the opportunity, just like normal cells, to increase (and restore) their number, a consequence of the induced cell death by ionizing radiation. In his article [ **33** ] , H. Rodney Withers described the processes of repopulation of tumor cells and that their rate of division after the initiation of radiation therapy is accelerated by up to 15-20 times compared to their rate before the initiation of treatment. The reason for this is thought to be that the factor accounting for how many cells after division processes die or cannot continue to divide - called cell-loss factor (CLF) - decreases in the course of radiation treatment. As an additional potential cause – the acceleration of the cell-division cycle due to reoxygenation processes in the tumor.

Here we will also mention the reverse process of repopulation, namely natural cell death. It is distinct from radiation-induced cell death and is a factor that should be considered in radiobiological modeling and the use of different TCP models.

- **Reoxygenation:**

Basically, the tumor is a conglomerate of cells with different radiosensitivity. As a rule, the cells located in the center of the tumor are radioresistant due to the fact that they lack a good blood supply and access to oxygen - the so-called hypoxic cells. This is due to the fact that the presence of oxygen contributes to the indirect damage/killing of tumor cells - by forming reactive oxygen species. The cells on the periphery, on the other hand, are richly supplied with blood and have better radiosensitivity to ionizing radiation - oxygenated cells [ **34** , **35** ] . During radiation therapy and between two consecutive irradiations - tumor cells can pass from a hypoxic to an oxygenated

state, because during irradiation, the most likely to die are the radiosensitive cells (those on the periphery) and thus access of oxygen to the cells located in the central parts of the tumor formation is ensured.

There are various mathematical models considering the dynamics of processes such as reoxygenation. It the study of Stavreva et al. [ **36** ] for example , the cells in the tumor are divided into two subgroups – oxic and hypoxic. The authors focused on resistant cells and their reoxygenation, an approach justified by the fact that they are more difficult to kill. In other studies [ **37** , **38** , **39** ], hypoxic cells were divided into acutely hypoxic and chronically hypoxic, and thus the subgroups became three.

The models of Stavreva et al. [ **36** ] and that of Ruggieri et al. [ **39** ] were used in the analysis [ **40** ] of the results reported in the article by Alite et al. [ **41** ], which analysis will be presented in **Chapter 5**.

- **Redistribution:**

Redistribution of cells within the cell-division cycle between individual fractions is an important factor in tumor response to fractionated radiation therapy [ **42** , **43** ].

The cell-division cycle goes through 4 phases:

- **G1** – cells from G0 phase can enter G1. This is the first phase of the cell-division cycle. The cell begins to grow and prepare to replicate the DNA. This phase lasts 3-24 hours. ( Gap phase 1).
- **S -** In order for one mother cell to produce two completely identical daughter cells, DNA copying is necessary and this happens in this phase. This phase lasts 6-8 hours.
- **G2 -** during this phase the cell prepares for the next phase - mitosis. This phase lasts 3-4 hours.
- **M** – the cell divides into two completely identical (daughter) cells. This phase lasts about 1 hour.

Tumor cells have different radiosensitivity depending on which phase of the cell cycle they are in during irradiation [ **44** , **45** , **46** , **47** , **48** ]. Cells in late S phase are usually the most radioresistant,

while cells in M phase and G2 phase are the most radiosensitive. It is this difference in radiosensitivity in the different phases of the cell cycle that is the basis of the idea of fractionation of radiotherapy.

- **Repair:**

Repair refers to the restoration (sub-lethal damage repair) of sub-lethal damage to the DNA chain caused by the passage of ionizing particles. It is known that healthy cells in the human body have a greater ability (than tumor cells) to recover after single-strand breaks as a result of passing ionizing particles through the DNA structure in the cell [ **31** , **49** ]. Fractionation of radiation therapy has shown great benefits for radiation therapy outcome [ **31** , **50** ] because the time interval between two consecutive radiations is the time that healthy but damaged cells have to undergo repair. The damage resulting from single-strand breaks in the DNA chain is valid for both healthy and tumor cells. Due to the property of healthy cells to recover between two irradiations with a higher probability than tumor cells, the benefits of fractionation outweigh the harms [ **51** , **52** ]. If the DNA damage resulting from the radiation is repaired so that we have a restoration of its functions, then it is called sublethal. Conversely, if its functions are not restored, the cell dies and then the damage is called lethal. Lethal damage, in turn, is divided into double-stranded breaks as a result of one particle simultaneously tearing both strands of DNA, and double-stranded breaks as a result of two independent events in a small time interval $dt$ , when two particles break one of the chains in a narrow section. It is these two modes of damage that are involved in the LQ model of cell damage with the parameters $\alpha$ and $\beta$ . The parameter $\alpha$ is associated with single-particle double-strand break, while $\beta$ is related to the breaking of the two chains by two separate particles.

## 3.1. Tumor Control Probability ( TCP )

The tumor control probability was first introduced by Munro et al. [ **53** ], as the probability of zero surviving tumor cells, since even one cell is sufficient for tumor regrowth.

First we need to divide the TCP models according to:

A) the conditions of irradiation:

- homogeneous TCP models – the entire tumor volume is considered to receive the same (prescribed) dose;
- heterogeneous TCP models – the dose distribution is non-uniform and we have different parts of the tumor receiving a different dose.

B) whether the reaction of:

- individual – individual TCP models;
- population – population TCP models.

At the beginning, the Poisson statistic is used to describe these processes [ **53** , **54** , **55** ], which is a borderline case of the binomial distribution.

In homogeneous irradiation up to dose $D$ and, accordingly, survival probability $p_s(D)$, the survival probability of $i$ tumor cells , $i \epsilon [\ 0,N\ ]$ after irradiation, is:

$$P(i,N) = C_N^i p_s^i (1-p_s)^{N-i} \quad (3)$$

$\boldsymbol{C_N^i}$ – binomial coefficient .

From where for zero surviving cells equation ( **3** ) becomes :

$$TCP = (1-p_s)^N \quad (4)$$

The Poisson model is an approximation of the binomial distribution, fulfilling the criteria: a large sample ( $N$ >50) and a small probability of an event ( $p_s$ <<1) . In this case, the number of cells is high ( $>10^3$ ) , and the probability of cell survival $p_s$ must be much less than unity:

$$TCP = P_0 = e^{-Ns} = e^{-Np_s} \quad (5)$$

where $N$ is the initial number of cells, $p_s$ is the cell survival probability , and $N_s$ is the mean number of surviving cells after irradiation.

In this model both parameters: repopulation rate, $\lambda$, and natural cell death, $\mu$, can be incorporated by solving : $\frac{dN}{dt} = \lambda N$ and $\frac{dN}{dt} = -\mu N$ :

$$N(t) = Ne^{\lambda T} \text{ , } N(t) = Ne^{-\mu T} \quad (6)$$

$N(t)$ is the number of cells at time $t$ , from where equation ( **5** ) becomes:

$$TCP = e^{-Np_s e^{\lambda T} e^{-\mu T}} \quad (7)$$

A major drawback of the Poisson model is the lack of time dependence. It cannot be used for arbitrary time intervals because only the parameter $T$, which is the total time of therapy, is involved in the equation. Another drawback is that repopulation, $\lambda$ , and natural cell death, $\mu$ , are involved in the equation as a difference, that is, with their net effect, which is a weakness of the model.

In 2000, Zaider & Minerbo [ **56** ] derived an analytical expression for the tumor control probability that is applicable to fractionated radiotherapy with arbitrary time intervals between fractions:

$$TCP(t) = \left[ 1 - \frac{(p_s(t)e^{(\lambda-\mu)t})}{(1+\lambda p_s(t)e^{(\lambda-\mu)t} \int_0^t \frac{dt'}{p_s(t')e^{(\lambda-\mu)t'}}} \right]^N \quad (8)$$

Formula ( **8** ) has been revised and presented for the cases of fractionated treatment with arbitrary time intervals between fractions in **Chapter 4.1 (** formula **15** ).

The TCP models presented so far in this chapter are individual TCP models valid for homogeneous irradiation.

For the first time, Fischer [ **57** ] considered the case of heterogeneous irradiation and the corresponding individual response. The tumor is divided into $n$ of number of tumorlets (sub-volumes) with volume $V_i$ - each irradiated homogeneously to a dose $D$. The TCP is calculated for

each sub-volume and the product of *the* $TCP_i(Vi)$ gives the tumor control probability after irradiating the entire volume. It is assumed that the events are independent, that is, the irradiation of a given sub-volume does not affect the others [ **58** ]. From which the equation has the form:

$$TCP_{ind} = \prod_{i=1}^{n} TCP(\rho(r_i)\delta V_i, D(r_i)) \quad (9)$$

where $\rho(r_i)$ is the clonogenic density, and $\rho(r_i)\delta V_i$ represents the number of cells in a small volume $\delta V_i$ around a point $r_i$ and $D(r_i)$ is the dose at that point. It is also considered that the parameters in the linear-quadratic model of cell killing ( $\alpha$ and $\beta$ ), as well as the repopulation, $\lambda$, are constant for the entire tumor. Thus, differential dose-volume histogram (dDVH) data from the planning system can be used to show the relative volume of the structure $V_i$ irradiated to dose $D_i$ : dDVH =$\{ V_i, D_i \}$ and equation ( **9** ) becomes:

$$TCP_{ind} = e^{\left[ -N_0 \sum_{i=1}^{n} V_i e^{-\left( \alpha + \frac{\beta D_i}{n_f} \right) D_i + \lambda T} \right]} \quad (10)$$

where $n_f$ is the number of fractions.

After summarizing the individual TCP models, we will also consider the population ones. Clinical data differ from experimental data in that we have a spread in radiobiological parameters among the population, because people are different and tumorigenesis proceeds differently in each patient. In 1993, Brenner DJ [ **59** ] first demonstrated the inability of an individual model to describe clinical (population) data after trying to fit an individual TCP model to clinical data and obtaining biologically unrealistic model parameter values. A year later, in 1994, Webb [ **60** ] repeated the analysis of the same clinical data, but using a population TCP model and reported the existence of an intra-parametric relationship between individual parameters ($\rho$ - clonogenic density, $\alpha$ - radiation sensitivity , $\sigma_\alpha$ _ – standard deviation , $V$ - volume and $D$ - dose ), which leads to the same values of the population TCP model. Intra-parametric correlation is eliminated in the work

of Carlone et al. [ **61** ] and all parameters are combined into two independent parameters – $D_{50}$ and $\gamma_{50}$ . These are the geometric characteristics of the "dose-response" curve ( TCP curve) indicating - the position of the curve, by $D_{50}$, which has the meaning of the dose leading to a 50% tumor control probability, and the slope of the curve, by $\gamma_{50}$ . Thus, the population model in the case of homogeneous irradiation has the form [ **61** ] :

$$TCP_{pop} = \frac{1}{2} erfc\left[\sqrt{\pi}\gamma_{50}\left(\frac{D_{50}}{D} - 1\right)\right] \quad (11)$$

where ***erfc*** is an additive function of the error.

In the case of a population model under heterogeneous irradiation Stavrev et al. [ **58** ] derive the formula:

$$TCP_{pop} = \frac{1}{(2\pi)^{3/2}\sigma_\alpha\sigma_\beta\sigma_\lambda}$$

$$\int_\alpha\int_\beta\int_\lambda e^{\left[-N_0\sum_i \nu_i e^{-(\alpha+\beta D_i/n_f)D_i+\lambda(T-T_k)}\right]} e^{\left(\frac{\alpha-\bar{\alpha}}{\sigma_\alpha}\right)^2+\left(\frac{\beta-\bar{\beta}}{\sigma_\beta}\right)^2+\left(\frac{\lambda-\bar{\lambda}}{\sigma_\lambda}\right)^2} d\lambda d\beta d\alpha \quad (12)$$

where $\bar{\alpha}$, $\bar{\beta}$,$\bar{\lambda}$ are the population means of the parameters $\alpha$ , $\beta$ and $\boldsymbol{\lambda}$ . $\sigma_\alpha$, $\sigma_\beta$, $\sigma_\lambda$ are respectively their standard deviations, assuming that the parameters in the population have a normal distribution. The authors prove (Figure **2 (b)** in their article) that the phenomenological individual model can be applied with great accuracy, in which only the geometrical parameters ( $\gamma_{50}$ , $D_{50}$ ) participate:

$$TCP_{ind/pop}^{geom} = 0.5^{\sum_i \nu_i \exp\left[\frac{2\gamma_{50}}{\ln 2}\left(1-\frac{D_i}{D_{50}}\right)\right]} \quad (13)$$

# 4. Dose-response assessment using TCP models, using data from animal experiments

Experiments with laboratory animals, in particular mice, have been used in the field of radiobiology for quantitative and qualitative assessment of the influence of different types of ionizing radiation on different types of tumors [ **62** , **63** , **64** ]. There are also in-vitro cell culture experiments [ **65** ] that can also serve to test different TCP models. The experiment of Fischer & Moulder [ **63** ] served to test the one mentioned in **Chapter 4.1** TCP model (equation **15** ) using the linear-quadratic model ( equation **2** ) and accounting for reoxygenation (equations **16** and **18**). Testing any TCP model is a necessity in order for it to be verified and subsequently used. Individual TCP models can be tested precisely on data from mouse experiments, because the mice used in the experiments are considered identical, that is, the tumors are assumed to develop similarly and the response to radiation is identical. In practice, an individual TCP model cannot and should not be used to quantitatively assess the outcome of a given treatment, because tumors in patients develop differently and at different rates, and in such a case population models should be used (were discussed in **Chapter 3.1**).

## 4.1. Fischer & Moulder data analysis

In Fischer's in-vivo experiment et al. [ **63** ], were irradiated laboratory mice that have been inoculated beforehand with a rare type of cancer – rhabdomyosarcoma. The irradiation schemes are 7 different fractionation modes – [ 1 3 5 7 10 15 22 ] fractions respectively for time [ 1 5 10 15 22 33 50 ] days . The treatment schedule is: Monday-Wednesday-Friday.

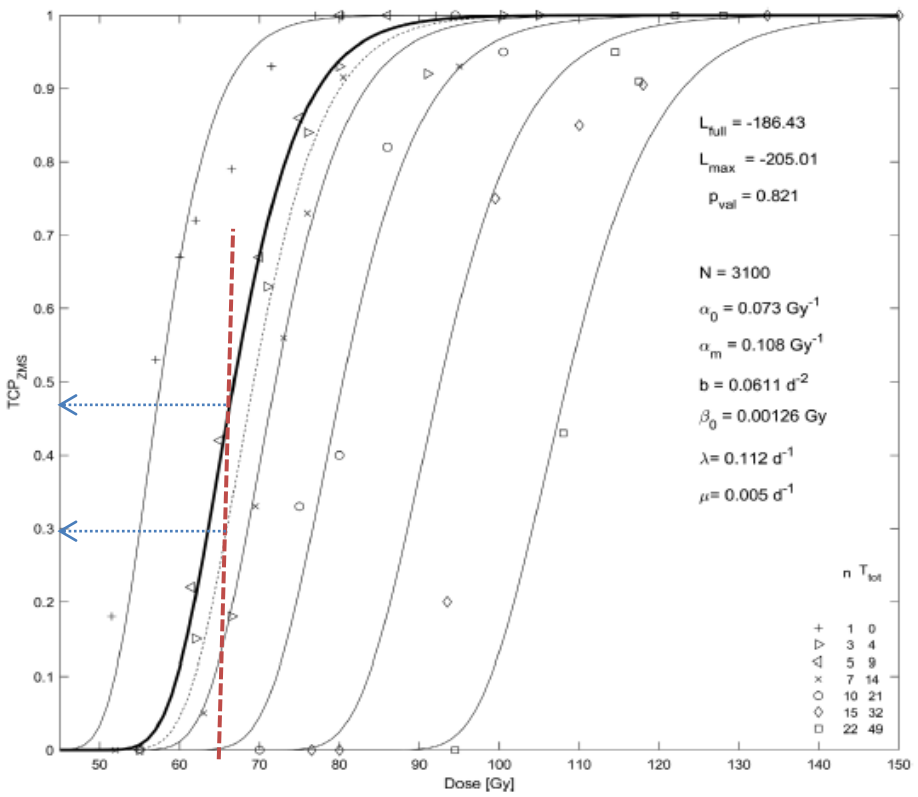


Figure 1 : Fit of Fischer and Moulder data with TCP $_{ZMS}$ the model

Two of the TCP curves in Figure **1** show inverse dose dependence relative to the others. These are the modes – 3 fractions for 5 days (3/5) and 5 fractions for 10 days (5/10). The curve (5/10) is to the left of (3/5). This phenomenon was explained by Stavreva et al. [ **36** ] with the process of changing the radiosensitivity (resensitization) of the cells during the treatment, due to the reoxygenation of the tumor. In the work of Stavrev et al. from 2018 [ **66** ] Fischer & Moulder 's data were analyzed including the process of natural (non-radiative) cell death of tumor cells. As a starting point, the TCP model of Zaider et al. [ **56** ] is used, which represents a solution to the infinite system of differential equations of Kendall [ **67** ] describing the processes of birth and death:

$$\frac{dP_i(t)}{dt} = (i-1)bP_{i-1}(t) - i[b+\delta]P_i(t) + (i+1)\delta P_{i+1} \quad (14)$$

In this equation, $\delta$ is a sum of radiation-induced and natural cell death, while $b(\lambda)$ is a parameter describing the process of cell division (birth) . The right-hand side of the equation represents a sum of probabilities for the processes that can lead to changes in $Pi(t)$ – as a result of division of any of the cells in state with (i-1) cells, by "disintegration" of the state with i cells as a result of division or death of any of i cells and as a result of death of any of the cells in state with i+1 cells.

Zaider's formula is a solution at i=0, since the concept of TCP is a probability of 0 surviving clonogenic cells. As a result the formula has been modified to be used for fractionated radiation therapy with random times between fractions, from Stavreva et al. [ **68** ]:

$$TCP(t) = \left[ 1 - \frac{p_s(t) e^{(\lambda-\mu)t}}{1 - \left( \frac{\lambda}{\lambda-\mu} \right) p_s(t) e^{(\lambda-\mu)t} \sum_{k=1}^{n-1} p_s^{-1}(T_{k-1}).\left[ e^{-(\lambda-\mu)T_k} - e^{-(\lambda-\mu)T_{k-1}} \right]} \right]^N \quad (15)$$

Where λ and μ account for repopulation and natural cell death, respectively, $P_s(t)$ is the cell survival probability, $t$ is the total time of the treatment course, $T_k$ and $T_{k-1}$ are the times immediately before and after a given fraction (irradiation), respectively, and N is the initial number of tumor cells. Formula ( **15** ) is valid when $p_s(T_{k-1})$ changes between fractions and for different models of cell killing.

A linear-quadratic model was used for the probability of cell survival after irradiation

To this LQ model, a parameter accounting for the reoxygenation of cells and, accordingly, their change in radiosensitivity during treatment will be added. The equation accounting for the change of $\alpha$ as a function of time was derived by Stavreva et al. [ **36** ]:

$$\alpha(t) = \alpha_0 e^{-a_0 t - \frac{b t^2}{2}} + \alpha_m \left( 1 - e^{-a_0 t - \frac{b t^2}{2}} \right) \quad (16)$$

where $a_0$ and $b$ are constants related to the increase in oxygen permeability of the outer layer of the tumor.$\alpha_0$ is the initial low radiosensitivity value, while $\alpha_m$ is the maximum value reached over time. $\beta$ in the specific case, it is assumed to be a constant, although it can be assumed that the two parameters change their value during the radiation treatment. Therefore, for the purposes of research in **Chapters 5** and **6** , we will also introduce here the equation to calculate the change of $\beta$ in the time.

An important parameter is the oxygen enhancement ratio (Oxygen Enhancement Ratio **)**, which represents the ratio of the dose given in an environment without oxygen to the dose given in an oxygen environment to achieve the same biological effect [ **69** ]. $\beta$ is assumed to be related to $\alpha$ via OER [ **40** ]:

$$OER = \frac{\alpha_m}{\alpha_0} = \sqrt{\frac{\beta_m}{\beta_0}} \quad (17)$$

where $\alpha_0$ and $\beta_0$ are the initial low values of the parameters and $\alpha_m$ and $\beta_m$ are the maximum values reached over time. This change in both parameters follows directly from the reoxygenation of hypoxic cells in the center of the tumor as a result of ionizing radiation and, accordingly, the increase in radiosensitivity as a function of time. We assume that for intermediate times (in the course of radiation treatment) there should be a relationship analogous to equation **17** , that is $\left( \frac{\alpha(t)}{\alpha_0} = \sqrt{\frac{\beta(t)}{\beta_0}} \right)$. Whence for $\beta\,(t)$ we have:

$$\beta(t) = \beta_0 \left( \frac{\alpha(t)}{\alpha_0} \right)^2 \quad (18)$$

In the study and data analysis of Fischer et al. [ **63** ], the data from the five irradiation regimes (excluding the two curves showing inverse dose effect (at 3 and 5 fractions)) were first fitted without considering the reoxygenation process using equations **2** and **15**. After that, all seven

curves were fitted taking into account reoxygenation (equations **16** and **18**). The method used to fit the experimental data with the investigated TCP model is by means of the maximum likelihood method [ **70** , **71** ]. A Monte Carlo technique was used to find the minimum of the deviation $D = -2(L_{fit} - L_{full})$ , where $L_{fit}$ is the maximum value of the log-likelihood of the best fit, while $L_{full}$ is the maximum value of the log-likelihood of the so-called „full" model in which the theoretical TCP values match the experimental values at each experimental point. Fischer et al. data are pooled in 12 animals per group. This allows the goodness of fit to be assessed by calculating the p-value of the fit. Assuming that the deviation $D$ has $\chi^2$ distribution, then the $p$-value is calculated:

$$p = \int_D^{\infty} f(x)dx \quad (19)$$

where $x = \chi^2_{df}$ is $\chi^2$-function for $df$ degrees of freedom.

$p$-values below 5% result in rejection of the $TCP$ model as failing to describe the experimental data. In Figure **2** can be seen $TCP_{ZM}$ model fit to the Fischer data and the parameters best describing the experimental data are shown ($\alpha$ , $\beta$ , $N$ , $\lambda$ and $\mu$):

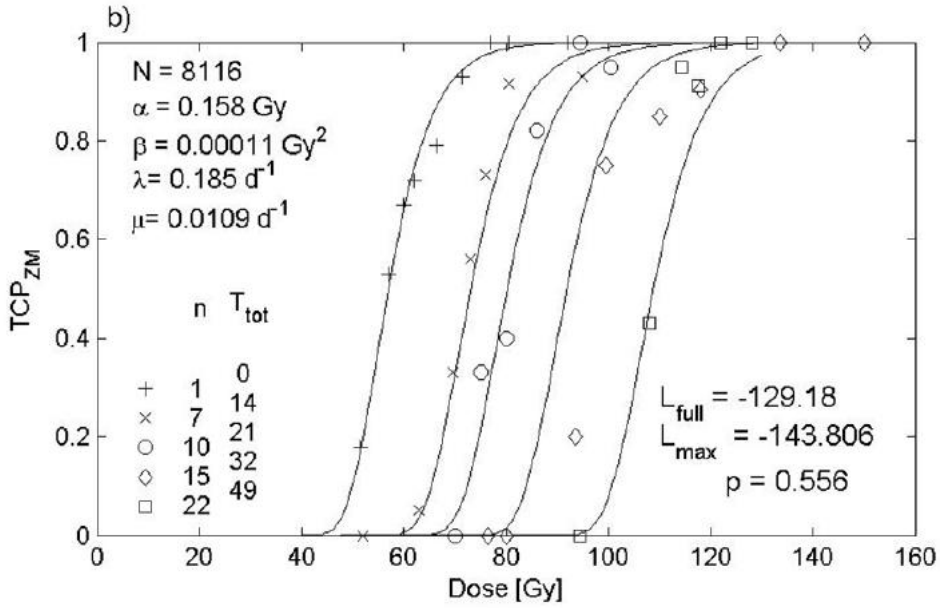


Figure 2 : Example fit of Fischer et al. data using TCP $_{ZM}$ model without including the two curves (3 and 5 fractions) that lead to inverse dose dependence.

An interesting correlation was found between the values of $\lambda$ and $\mu$ and more precisely in their net effect expressed in the difference between the two values. Pairs of $\lambda$ and $\mu$ parameter values were selected, which lead to an equally good fit to the data (*Lfit ∈ [ 143.8 0 61 , –143. 7984 ]*), and the dependence $\lambda(\mu)$ was constructed. We conclude that there are an infinite number of such pairs of parameters, all arising from fits with close values (shown in Figure **3**):

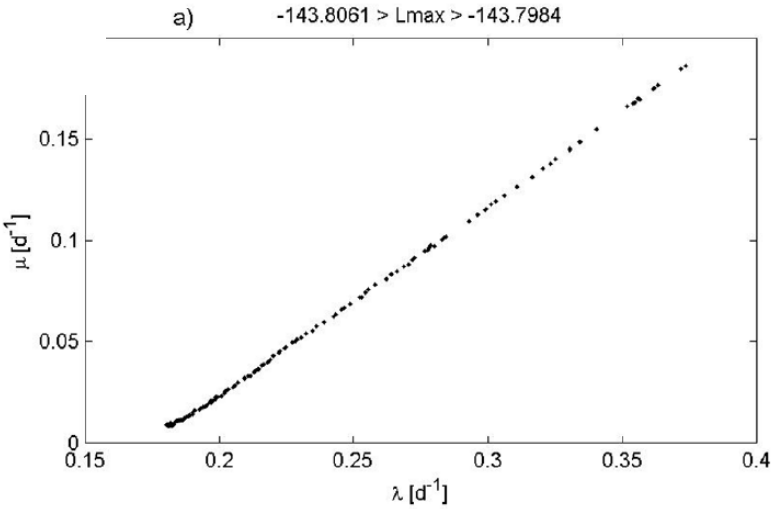


Figure 3 : Pairs of parameters $\lambda$ and $\mu$, leading to an equally good fit to the data of Fischer et al., using $TCP_{ZM}$ model without including the two curves (3 and 5 fractions) that lead to inverse dose dependence.

The following is a fit of the complete data set from the Fischer et al. experiment, including the seven TCP curves. This time, reoxygenation is also taken into account in the TCP model (equations **16** and **18**). The data is presented in the following figure:

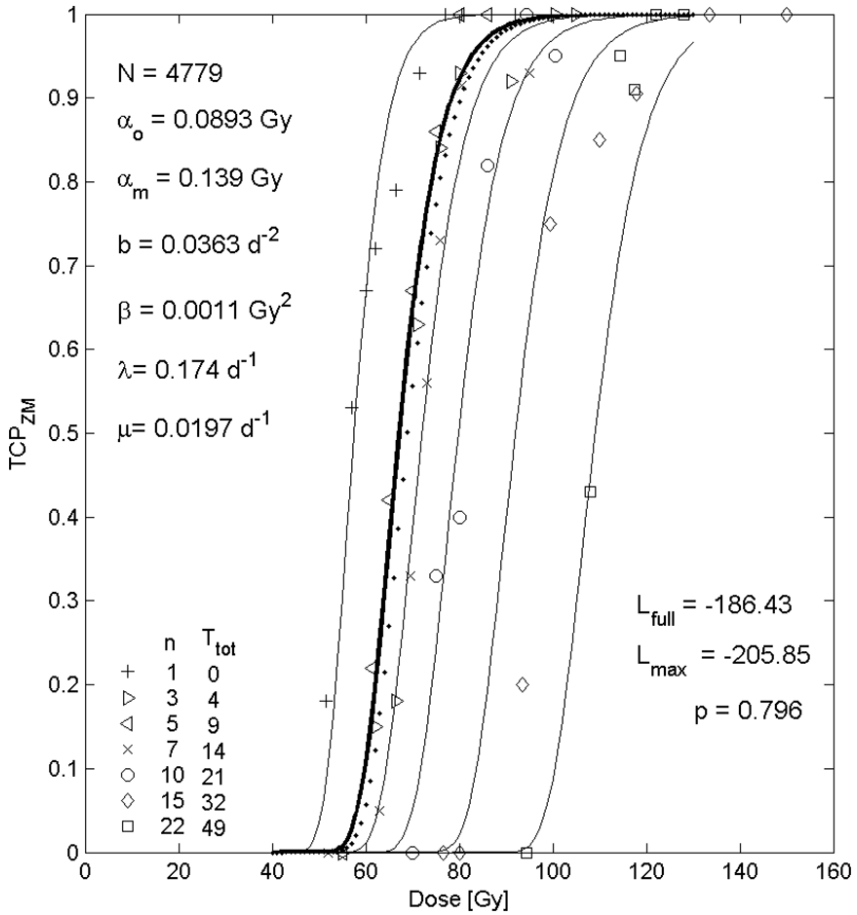


Figure 4 :A fit of $TCP_{ZM}$ model, including reoxygenation, to the full data set of the Fischer & Moulder experiment.

It was investigated the influence of $\lambda$ and $\mu$ on *TCP* using equation ( **15** ) and for different pairs of parameters $\lambda$ and $\mu$, so that their difference $\Delta=(\lambda-\mu)$ is equal. A difference in the calculated *TCP* values was found and depended mainly on $\Delta$ and the number of fractions. The differences range from 1-2% to about 10%. At $\mu$=0.13$d^{-1}$ and $\mu$=0$d^{-1}$ the *TCP* difference was 10.2% (30 fractions and 3 Gy per fraction). The observed correlation between the two parameters describing the birth and death rates suggests that even in this model, where the two processes are loosely separated, quite diverse data sets would be needed to estimate the two effects separately. The weak separation can be explained by the fact that in equation ( **15** ) there is only one place where the parameter $\boldsymbol{\lambda}$ participates alone. Everywhere else participates as a difference – $(\lambda-\mu)$.

## 4.2. Tarnawski et al. data analysis

In their in-vitro experiment, Tarnawski et al. [ **65** ] irradiated mega-colonies of two types of cells using 3 fractional regimens – single (acute) irradiation, daily irradiation (Monday-Sunday) and every working day (Monday-Friday). Fractional regimens are delivered at 2 Gy per fraction. The data were fitted using equation ( **15** ) and the method described in **Chapter 4.1**. Fit results for both types of mega-colonies were identical, so only those from A549 cells are shown (human lung adenocarcinoma cells). Tarnawski's data were also grouped, like those of Fischer et al., into 9 mega-colonies per group, allowing goodness of fit to be assessed by calculating the $p$-value using equation ( **19** ). The results here also show a strong dependence between $\lambda$ and $\mu$, seen in the following figure:

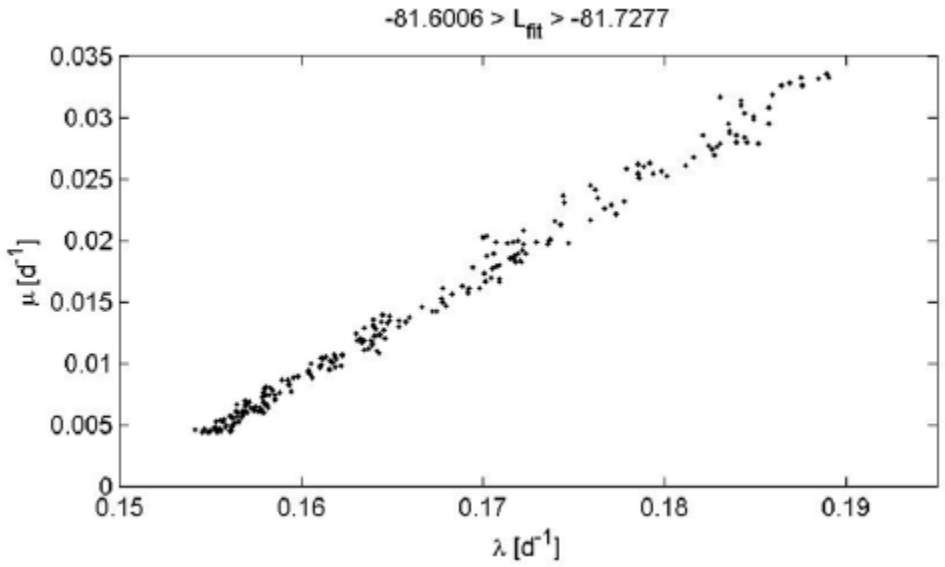


Figure 5 : Pairs of parameters $\lambda$ and $\mu$ leading to an equally good fit to Tarnawski et al. data using $TCP_{ZM}$ model.

A plot of the Tarnawski data, fitted using equation ( **15** ), is shown in Figure **6**:

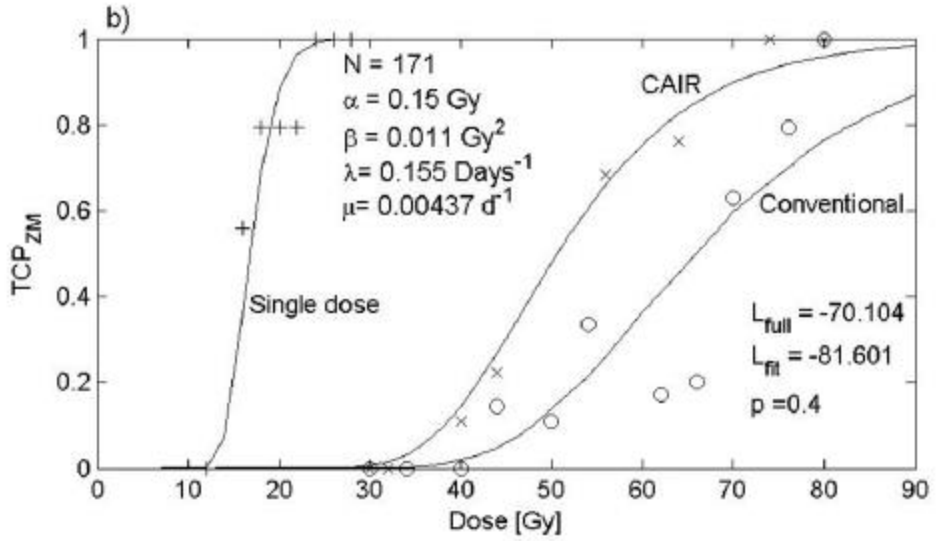


Figure 6 : Example fit of Tarnawski et al. data using $TCP_{ZM}$ model.

## 5. Changing the radiation treatment pattern and its impact on the tumor control probability

In this chapter, a theoretical study was carried out, inspired by the clinical results obtained in the article by Alite et al. [ **41** ] reporting the achievement of tumor control with different SBRT regimens: the conventional one - 1-5 fractions realized on consecutive days (Saturday and Sunday - rest), and the extended one - 1-5 fractions implemented in a Monday-Wednesday-Friday scheme (Saturday and Sunday - rest). In their article, Alite et al. reported that SBRT therapy in five fractions delivered on nonconsecutive days resulted in better local control and similar toxicity compared to radiation on five consecutive days.

TCP models are used, in which the reoxygenation of the cells during the radiation treatment is taken into account:

a) **The first** model is the Zaider-Minerbo-Stavreva model (ZMS), which represents a solution to the equation of Zaider et al. [ **56** ] in the case of fractionated radiotherapy with arbitrary time intervals between fractions ( formula **15** ) and taking into account the reoxygenation of tumor cells

( formula **16** ). In this TCP model, the linear-quadratic model of cell survival is modified to account for reoxygenation of the tumor during treatment.

It should be noted that although in this model, the presence of two subpopulations of cells is assumed - one in a hypoxic state (radioresistant) and the other in an oxygenated state (radiosensitive), we use the equations ( **2** , **15** , **16** and **18** ) to describe the reaction of a single-component radiosensitivity tumor irradiated homogeneously. This is justified due to the fact that number of articles [ **54, 72, 73** ] showed that the treatment outcome of a tumor heterogeneous in radiosensitivity is mainly determined by its hypoxic subpopulation.

Three different fractionation regimes are compared. They deliver the same dose per fraction in the same number of fractions, but the time between fractions (and total therapy time) differs. The first regimen is the one used in the Fischer et al. experiment, namely 5 fractions in 10 days (Monday-Wednesday-Friday-Monday-Wednesday). The second is the conventional one - from Monday to Friday (5 days). The third is the one used in the clinical trial by Alite et al. – Monday-Wednesday-Monday-Wednesday-Monday (total 15 days). The methodology for ranking radiotherapy plans, by comparing the probabilities of tumor control obtained for different plans and at different values of the radiobiological model parameters, is discussed in detail in [ **74** ].

In order to verify the validity of the modifications described above (equations **17** and **18**), the proposed model was fitted to the experimental data of Fischer et al., by a method already mentioned in **Chapter 4.1** and described in detail by Stavrev et al. [ **71** ]. The result is p-value = 0.821, which is as good as the result obtained by Stavrev et al. [ **66 ] (** p-value 0.796) – see figure **4** in **Chapter 4.1**. Since it is more logical that the two parameters, $\alpha$ and $\beta$, increase with time due to the reoxygenation processes, the further investigation was carried out, based on the acceptance of the concept that $\beta$ also increases over time. The resulting parameters from the fit best describing the Fischer et al. data are shown in Figure **7**:

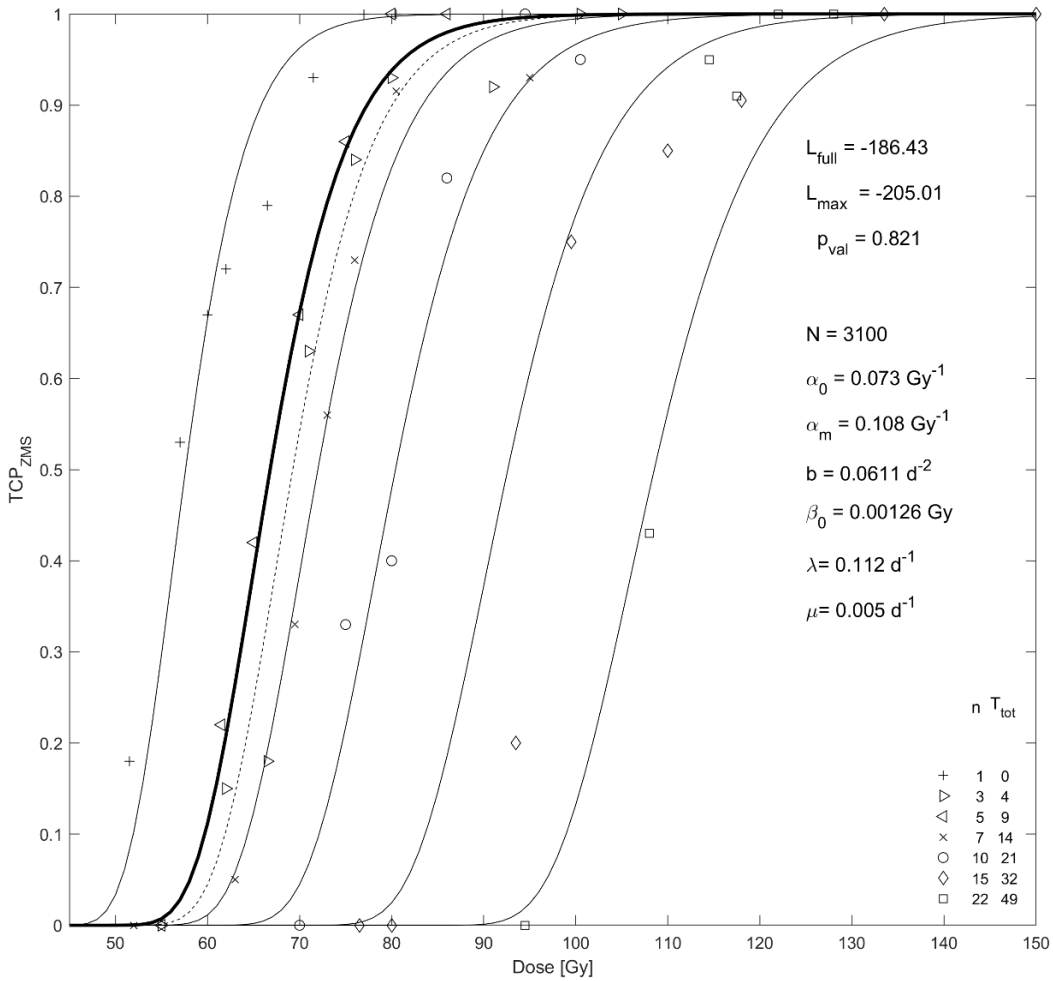


Figure 7 : Fit of the modified ZMS model to the Fischer and Moulder data

From the above figure it can be seen that the values of the parameters $N$ , $\lambda$ , $\mu$ , $\alpha_0$ , $\alpha_m$ are lower than those obtained in **Chapter 4.1** ( figure **4** ). The lower values are due to the fact that taking reoxygenation into account, already $\beta(t)$ is not a constant and changes over time, as well as $\alpha(t)$, through the dependence described in equation ( **18** ). Again, the initial cell count was low ($N$ =3100) because it corresponded to the number of hypoxic cells in the subpopulation. The value of $\beta_m$ calculated by formula ( **18** ) is 0.0028 Gy $^{-2}$ , and OER= $\alpha_m / \alpha_0$ =1.48.

Once we have found the parameters that best describe the experimental data of Fischer et al. , it follows to calculate the TCP using equations ( **2** , **15** , **16** and **18** ), for the three fractional regimes. Two cases with different input parameters are considered, the first being:

- 5 fractions and dose per fraction $d_f$ = 15 Gy:

TCP values are presented in Figure **8a** as a 2D function of the parameters $\lambda$ and $b$, and compared the Fischer mode (5 fractions in 10 days) with the 5 fractions in 5 days (Monday to Friday) mode. The intervals of the model parameters, $\lambda$ and $b$, are respectively ( $\lambda \in [\ 0.01, 0.2\ ]d^{-1}$ ) and ( $b \in [\ 0.01, 0.15\ ]d^{-2}$ ), and contain the intervals of values of each of the two parameters that result in an equally good fit to the experimental data. Accordingly, the difference of the TCP values of the two modes, for a set of pairs of parameters ( $\lambda$ and $b$ ), was calculated and constructed the corresponding isolines (figure **8c** ) corresponding to a fixed value of the difference $\Delta$ TCP = $TCP_{1,3,5,8,10} - TCP_{1,2,3,4,5}$ ( the indices indicate the day of the corresponding fraction), as $\Delta$ TCP varies from 0% to 40%. In a very small interval of the parameter space, a negative value of $\Delta$ TCP is observed , but this can be ignored, as it is in a region where in practice both TCPs tend to 0, which is a clinically unacceptable result.

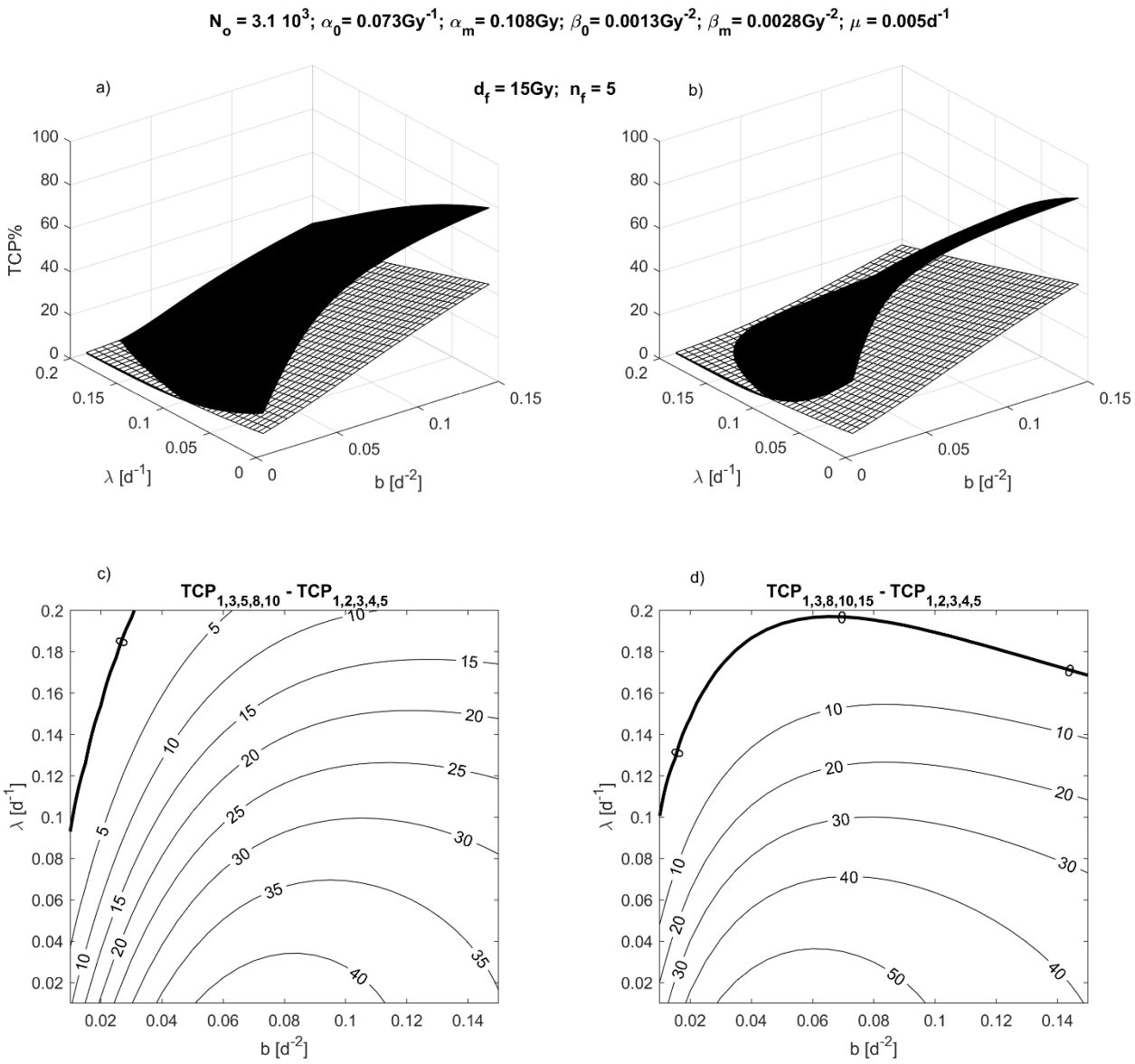


Figure 8 TCP as a 2 D function of the parameters $\lambda$ and $b$ , at dose per fraction $d_f$ =15Gy. The TCP surface of the extended modes (5 fractions in 10 days (5/10) / 5 fractions in 15 days (5/15)) is shown in black. In fig. 8a compares the 5/10 and 5/5 modes, and in fig. 8b – 5/15 and 5/5. Figures 8c,d show the isolines of Δ TCP in the plane ( $\lambda$ and $b$ ), respectively, for both cases: $TCP_{1,3,5,8,10} - TCP_{1,2,3,4,5}$ and $TCP_{1,3,8,10,15} - TCP_{1,2,3,4,5}$ .

The same study was conducted to compare and the regimen used by the Alite et al. article (5 fractions in 15 days) versus conventional. The results are presented in figure **8 b**,**d** . Here we have Δ TCP values reaching up to +50% in favor of the extended mode. What was observed is that in 12% of the cases we have a negative value of Δ TCP (up to -7%), which corresponds to a better

prognosis for the outcome of radiotherapy in the short regimen (5 fractions in 5 days). However, in only 2% of the total number of cases considered, we have a significant negative difference for Δ TCP (between -5% and -7%). It should also be noted that this negative difference is observed in the region with low TCP values ($TCP_{max}$ <20%) – values that are not clinically significant.

The second therapeutic regimen considered is:

- 5 fractions and dose per fraction $d_f$ =11.5Gy:

In this case, we change the input parameters so that the ratio $\alpha/\beta$ at the beginning of the irradiation, that is, $\alpha_0/\beta_0$ should be equal to 10 - values reported in [ **75** , **76** ]. Then for $\beta_m$ it is obtained (through formulas **16** and **18** ): $\beta_m$ =0.024 $Gy^{-2}$, from where $\alpha_m/\beta_m$ = 7.9Gy, OER= $\alpha_m/\alpha_0$ =1.27. The assumed strong dependence of the $\beta$ mechanism, as well as the higher values of $\alpha_0$=0.15$Gy^{-1}$ and $\alpha_m$=0.19$Gy^{-1}$ (compared to the previous case, where $\alpha_0$ = 0.073$Gy^{-1}$ and $\alpha_m$ = 0.108$Gy^{-1}$), allow the achievement of acceptable values for TCP in the used fractional modes with a dose per fraction $d_f$ =11.5Gy and with a much larger number of initial hypoxic tumor cells. This dose fraction was used clinically by Alite et al. The results are presented in figure **9**, and again we have the advantage of the two extended regimes (of Fischer et al. (5 fractions in 10 days) and of Alite et al. (5 fractions in 15 days)) compared to conventional – 5 fractions in 5 days, reaching values of $\Delta TCP_{Fischer} = TCP_{1,3,5,8,10} - TCP_{1,2,3,4,5}$=30% and $\Delta TCP_{Alite} = TCP_{1,3,8,10,15} - TCP_{1,2,3,4,5}$=40%.

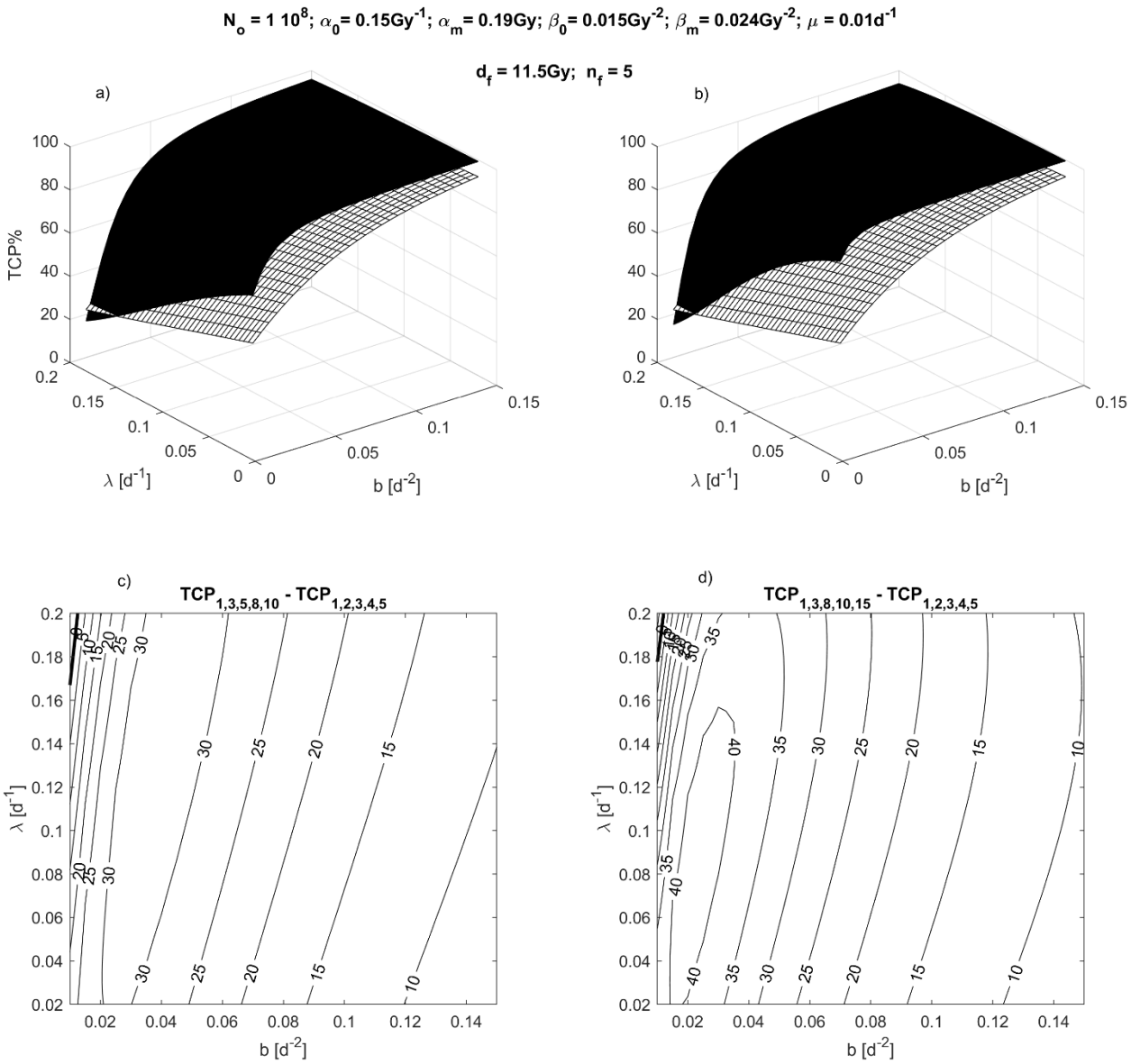


Figure 9 . TCP as a 2D function of parameters λ and b, at dose per fraction df=11.5Gy. The TCP surface of the extended modes (5 fractions in 10 days (5/10) / 5 fractions in 15 days (5/15)) is shown in black. In fig.9 a compares the 5/10 and 5/5 modes, and in fig.9b – 5/15 and 5/5. Figures 9c,d show the isolines of ΔTCP in the plane (λ and b), respectively, for the two cases: $TCP_{1,3,5,8,10} - TCP_{1,2,3,4,5}$ and $TCP_{1,3,8,10,15} - TCP_{1,2,3,4,5}$.

Again, a section of the parametric space is noticed where we have a slight advantage of the conventional mode over the other two (figure **9a**,**b**), but this difference is below -5% for the Fischer et al. mode and below -7% for the Alite et al. mode. Again, this abnormal dependence is observed in a region with low TCP values of the order of ≈20%, which again are not clinically relevant

values. However, if a higher value of $\alpha_m$ is assumed, the absolute advantage of extended modes is observed throughout the parametric space considered, but this will not be shown graphically.

In **conclusion**:

The higher $\alpha_m$ values for a given value of $\alpha_0$ favors the extended modes over the conventional one, since thus in most cases (it depends on the value of the parameter b) the shorter therapy time is not enough for the radiosensitivity to reach its maximum value and thus to have a full advantage of the resensitization itself.

An interesting result is the larger value of $\Delta\ TCP_{Alite} = TCP_{1,3,8,10,15} - TCP_{1,2,3,4,5}$ ( Alite mode vs conventional mode) vs $\Delta\ TCP_{Fischer} = TCP_{1,3,5,8,10} - TCP_{1,2,3,4,5}$ ( Fischer mode vs. conventional mode) in all examples considered. At the same time, and with the observed negative values of $\Delta$ TCP in both comparisons - again the "advantage", although negative, is in the Alite regime over that of Fischer ($\Delta\ TCP_{Alite} > \Delta\ TCP_{Fischer}$) .

b) **The second** model that will be considered and used to evaluate the different fractionation modes in the SBRT radiation technique is the Ruggieri-Nahum (RN) model. In this TCP model, described in several papers [ **39** , **77** , **78** ], the tumor is considered as a conglomerate of cells with different radiosensitivity and accordingly divided into three groups – oxygenated cells, acutely hypoxic and chronically hypoxic. Each of these sub-populations of cells is characterized by its own values of the parameters determining their radiosensitivity, $\alpha$ and $\beta$, involved in the LQ model of cell killing.

Well-oxygenated cells divide continuously, while acutely hypoxic cells are part of the time ( $C$ ) in a hypoxic state, and the other part of the time ( $1\text{-}C$ ) – in an oxic state. During the time acutely hypoxic cells are in an oxic state, their radiosensitivity is like that of well-oxygenated cells and they also divide like them. Chronically hypoxic cells they do not divide, but can go from a hypoxic to an oxic state during radiation therapy. The fraction of cells that reoxygenates (goes from a hypoxic to an oxic state) is considered as a function of time: $B(t) = 1 - e^{-at}$ . Due to the complex

interrelationship between the three cellular components (oxic, acutely and chronically hypoxic cells), the simplified Poisson TCP model was used to calculate the tumor control probability:

$$TCP = e^{-N_s} = e^{-\left(N_o^n + N_{ah}^n + N_{ch}^n + \tilde{N}_o^n\right)} \quad (20)$$

where $N_o^n$ is the mean number of surviving oxic cells, $N_{ah}^n$ - acutely hypoxic, $N_{ch}^n$ - chronically hypoxic , $\tilde{N}_o^n$ - chronically hypoxic, transformed into oxic cells, after n number of irradiations. Correspondingly, $N_s$ is the total number of surviving cells (hypoxic and oxic).

We used the parameter values obtained by Ruggieri et al. [ **39** ] in fitting the data of Fischer and Moulder [ **63** ]. TCP values were calculated for the two irradiation regimes and are presented as a 2D function of the parameters $C$ and $a$, for different values of the remaining model parameters and for two different values of dose per fraction. The parameters $C$ and $a$ are in the interval: $C \in [0,0.4]$ and $a \in [0,0.15]\text{d}^{-1}$, so as to cover the values obtained by Ruggeri et al. The choice to study the dependence of the radiation treatment outcome on these two parameters in particular ( $C$ and $a$ ), is due to the fact that the parameter $C$ determines the oxygen status of the acutely hypoxic component, and the parameter $a$ determines the rate of reoxygenation of chronically hypoxic cells. The idea here again is that the outcome of radiation therapy is thought to depend primarily on the killing of the hypoxic tumor cell conglomerate, from which it is logical to assume that it is these two parameters that would have the greatest impact on TCP.

Analogously to the study with the ZMS model, for the RN model we will compare the conventional mode (Monday to Friday) - with that of the article by Fischer et al. (Mon-Wed-Fri-Mon-Wed) and that of the article by Alite et al. (Mon-Wed-Mon-Wed-Mon), for the following SBRT cases:

- 5 fractions and dose per fraction $d_f = 11.5$ Gy:

The results are presented in Figure **10**:

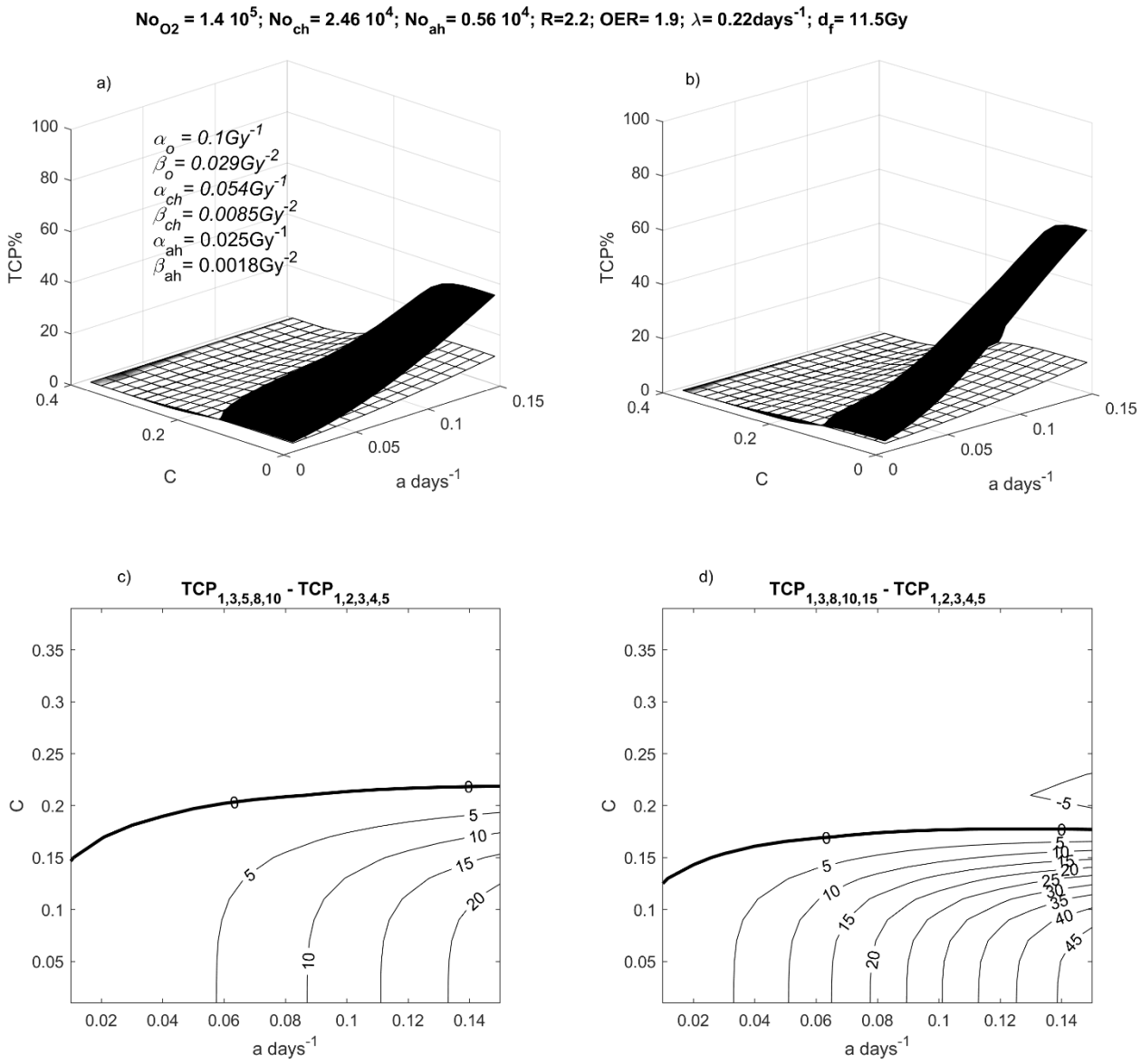


Figure 1 0 : TCP calculated according to the model of Ruggieri & Nahum, as a 2D function of the parameters C and a , at a dose per fraction $d_f$=11.5Gy. The rest of the parameter values were obtained and taken from the article by Ruggieri et al. [ **39** ]. The TCP surface of extended modes (5 fractions in 10 days (5/10) / 5 fractions in 15 days (5/15)) is shown a in black. In fig.10a compares the 5/10 and 5/5 modes, and in fig . 1 0 b – 5/15 and 5/5. Figures 10c,d show the isolines of ΔTCP in the plane (C and a), respectively, for the two cases: TCP $_{1,3,5,8,10}$ – TCP $_{1,2,3,4,5}$ and TCP $_{1,3,8,10,15}$ – TCP $_{1,2,3,4,5}$ .

TCP values reaching 20% in favor of the Fischer & Moulder mode and up to 45% in favor of the regime of Alite et al. Again, there is a small region of the parametric space (about 2% of the cases) where the conventional mode gives better results for TCP than the Alite mode, reaching a

difference of Δ TCP =(-5%). However, this difference in favor of the conventional regimen is at very low (for both regimens) calculated TCP values, on the order of 10%, which are not clinically relevant values. In the Fischer & Moulder mode, the maximum TCP values obtained are around 30%, which is also too low and would not be acceptable in practice. On the other hand in Alite et al. mode this maximum value is larger and reaches about 60%, but it is in a small part of the parametric space - where we have low values of the parameter $C$ and high values of $a$.

The second therapeutic regimen considered is:

- 5 fractions and dose per fraction $d_f$ = 15 Gy:

Due to unsatisfactory TCP values at 11.5 Gy per fraction, a case with a higher dose – 15 Gy per fraction was considered. The remaining model parameters remain unchanged. Contrary to the initially expected result - here we have an advantage of the short mode, compared to the two extended modes, and for all considered values of $C$ and $a$. The results are presented in figure **11**:

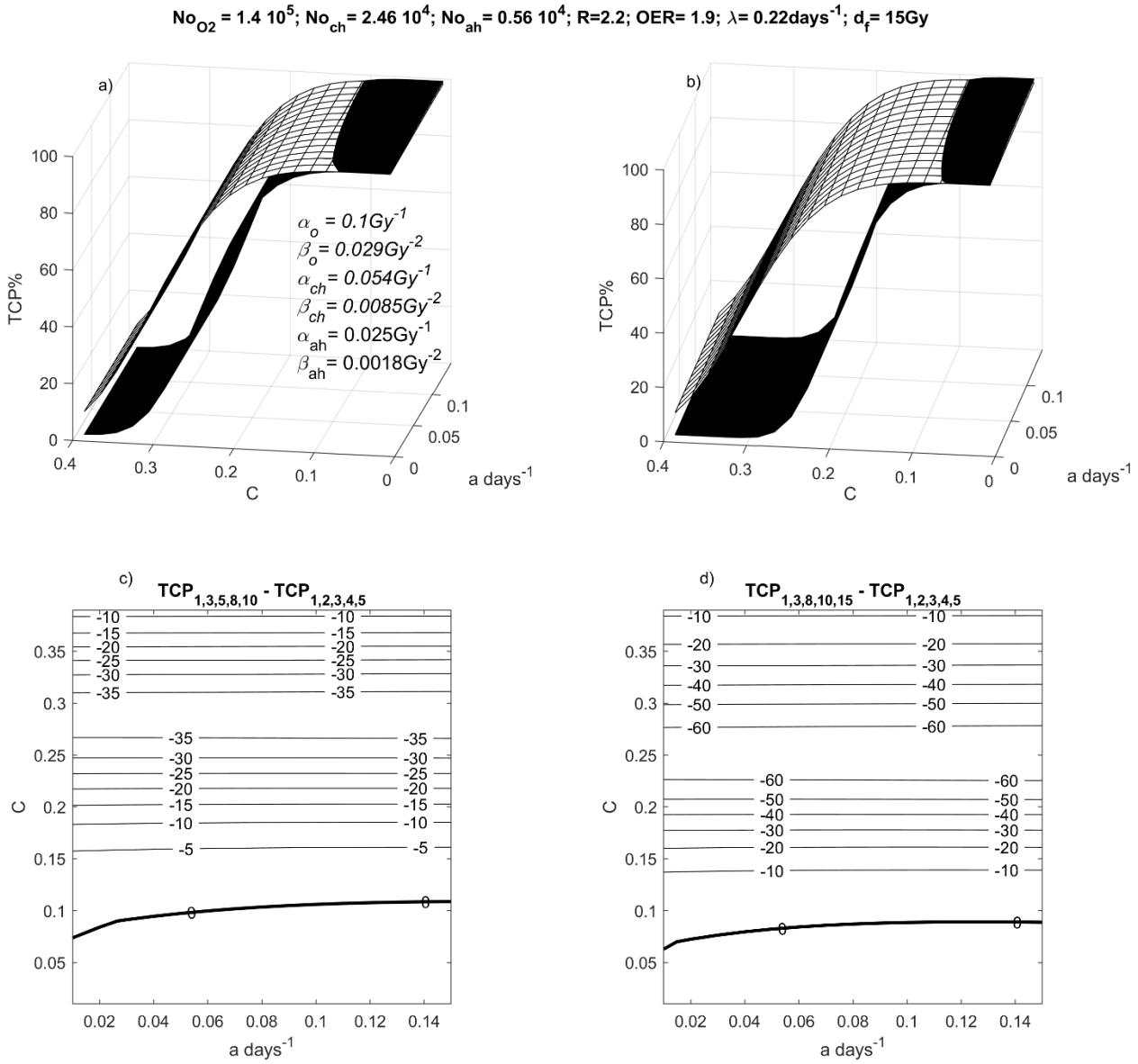


Figure 11 : TCP calculated according to the model of Ruggieri & Nahum, as a 2D function of the parameters C and a , at a dose per fraction df=15Gy. The rest of the parameter values were obtained and taken from the article by Ruggieri et al. [ **39** ]. The TCP surface of extended modes (5 fractions in 10 days (5/10) / 5 fractions in 15 days (5/15)) is shown a in black. In fig.11 a compares the 5/10 and 5/5 modes, and in fig.11b – 5/15 and 5/5. Figures 11c,d show the isolines of ΔTCP in the plane ( C and a ), respectively, for the two cases: $TCP_{1,3,5,8,10} - TCP_{1,2,3,4,5}$ and $TCP_{1,3,8,10,15} - TCP_{1,2,3,4,5}$

In the first case Δ TCP= $TCP_{1,3,5,8,10} - TCP_{1,2,3,4,5}$ reaches (-35%), and in the second Δ TCP = $TCP_{1,3,8,10,15} - TCP_{1,2,3,4,5}$ reaches up to (-60 %). An interesting finding can be seen from the above

figure – parameter $a$ has no effect on TCP and treatment outcome, which means that reoxygenation of chronically hypoxic cells has no effect on TCP at all three time regimes.

## 6. Effect of dose uncertainty on the tumor control probability

This theoretical study is necessary due to the fact that dose delivery to the tumor has uncertainty caused by factors such as - calibration of the radiotherapy machine (output of the machine, field profiles), position of the "leafs" of the multileaf collimator (MLC) in each moment during the procedure (applies to techniques with intensity modulation – IMRT, VMAT), the calculation algorithms of the planning system. These are machine-related uncertainties, but there are also human-related uncertainties – correct delineation of the planning target volume (PTV) and critical organs (OAR), movement of the tumor and critical organs during irradiation, table position, immobilization devices, correct matching of a 3D image obtained by means of CBCT ( Cone Beam Computed Tomography) immediately before irradiation, with that of the CT scanner, on which the 3D image of the dosimetric plan itself was prepared.

In the case of the cylindrical ionization chambers of PTW dosimetry, those that are widely used for absolute dosimetry (when calibrating the devices) of high-energy X-ray beams are Farmer type. They are waterproof to enable measurements to be carried out in a water phantom, where equilibrium of the secondary charged particles is achieved, under reference conditions. The reported uncertainty of the dosimetric system used in dosimetric measurements of radiotherapy equipment is of the order of 1.5% [ **6** , **12** ]. It is reported to measure the water dose $D_{w,Q}$ from high-energy photon radiation, at a reference depth in a water phantom and using an ionization chamber calibrated in $^{60}$Co gamma radiation. As the combined relative standard uncertainty is the sum of the relative uncertainty associated with the calibration of the camera in a secondary standard dosimetry laboratory (SSDL), which is 0.6%, and the relative uncertainty associated with the dose measurement itself under reference conditions in the phantom, which is 1.4%. The combined relative uncertainty is estimated at 1.5%. If the calibration of the dosimetric system is performed in a primary standard dosimetry laboratory (PSDL), this uncertainty is of the order of 1.2%. Thwaites [ **79** ] in his publication reported the uncertainty of the dose relative to the reference

value of the dose delivery itself in the patient, by means of in-vivo dosimetry. Deviations vary between 1.6% - 3.2%.

Since the study [ **80** ] is theoretical, a program written in Matlab was created, which considers cases of deviations of the delivered dose from the reference (prescribed) within wide limits – from 1% to 10%. Cases of conventional Monday-Friday radiation and hypofractionated radiotherapy with high dose per fraction (SBRT, SRS) were reviewed. TCP values were calculated according to formula ( **15** ), taking into account the reoxygenation process. 10,000 iterations were run with varying dose per fraction. This dose variation is normally distributed around the true dose value. In Figures **12** and **13** histograms of the tumor control probability corresponding to the corresponding prescribed dose are presented:

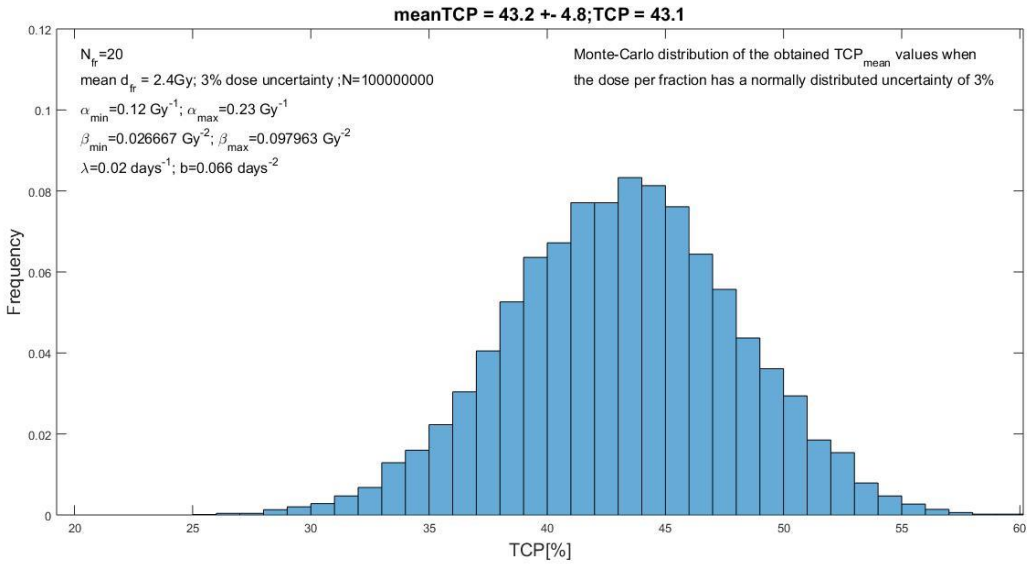


Figure 12 : Histogram of the distribution of TCP values as a function of frequency, at a dose uncertainty of 3%. Mode: from Monday to Friday. Fractionation: 20x2.4Gy

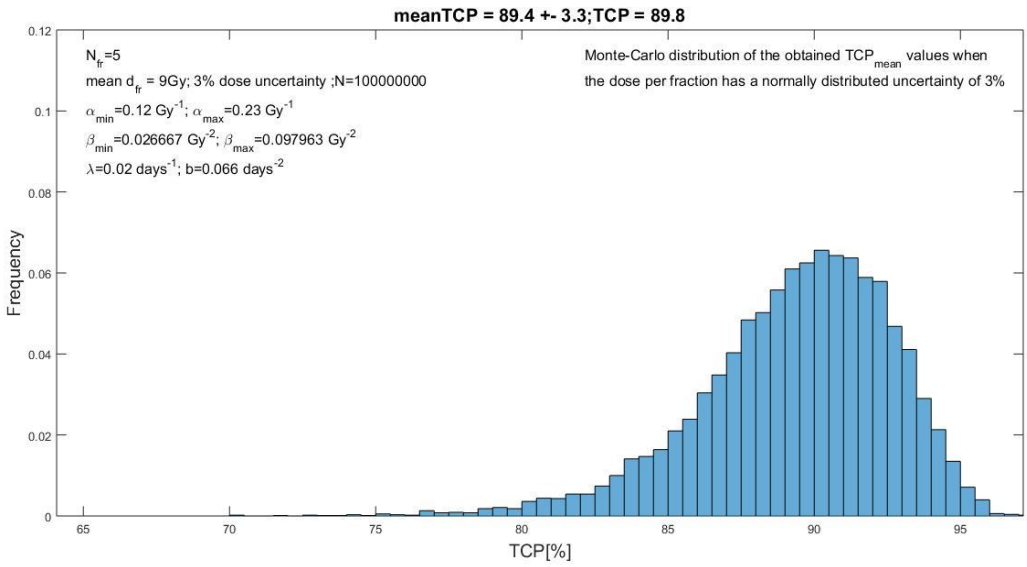


Figure 13 : Histogram of the distribution of TCP values as a function of frequency, at a dose uncertainty of 3%. Mode: from Monday to Friday. Fractionation: 5x9Gy

The input parameters ( $\alpha_{min}$ , $\alpha_{max}$ , $\beta_{min}$ , $\beta_{max}$ , b, $N$, $\lambda$ ) are not random but taken from [ **81** ] and correspond to prostate carcinoma irradiation.

Figures **12** and **13** show a large scatter of results for TCP. In the case of irradiation 20x2.4Gy ( figure **12** ) – we have an average value of TCP [ 43.2±4.8 ] % ( uncertainty is 1σ ), with a minimum value of 25.3% and a maximum of 60.3%. At 5x9Gy (figure **13** ) – we have an average value [ 89.4±3.3 ] %, with a minimum value of 70.4% and a maximum of 97.2% .

The conventional fractional modes considered are as follows: 20x2.4Gy | 23x2.12Gy | 25x2Gy | 30x2Gy , and the hypofractionated regimens are: 3x15 Gy | 4x10Gy | 4x11Gy | 5x9Gy and 5x10Gy. They are presented in table 1:

| Dose prescription | TCPmean ± 1$\sigma$ (%) | | | $TCP_{ZMS}$ (%) |
|---|---|---|---|---|
| | 3% | 5% | 10% | |
| *Conventional* | | | | |
| 20 × 2.4 Gy | 43.21 ± 4.75 | 43.46 ± 7.01 | 43.51 ± 13.57 | 43.09 |
| 23 × 2.12 Gy | 25.46 ± 4.09 | 25.71 ± 5.98 | 27.18 ± 11.63 | 25.25 |
| 25 × 2 Gy | 30.76 ± 4.04 | 30.83 ± 5.96 | 32.04 ± 11.52 | 30.57 |
| 28 × 2 Gy | 90.34 ± 1.09 | 90.31 ± 1.67 | 90.18 ± 3.41 | 90.35 |
| 30 × 2 Gy | 98.08 ± 0.24 | 98.08 ± 0.36 | 98.02 ± 0.76 | 98.09 |
| *SBRT* | | | | |
| 3 × 15 Gy | 99.90 ± 0.06 | 99.88 ± 0.11 | 99.73 ± 0.64 | 99.91 |
| 4 × 10 Gy | 24.82 ± 10.36 | 25.83 ± 14.63 | 29.73 ± 24.67 | 24.01 |
| 4 × 11 Gy | 94.20 ± 2.13 | 93.75 ± 3.53 | 91.49 ± 9.69 | 94.50 |
| 5 × 9 Gy | 89.38 ± 3.26 | 88.93 ± 5.15 | 86.10 ± 12.79 | 89.80 |
| 5 × 10 Gy | 99.81 ± 0.08 | 99.79 ± 0.14 | 99.67 ± 0.55 | 99.82 |

Table 1 : Comparison of the resulting TCP values when applying 3, 5 and 10% uncertainty, as well as the calculated $TCP_{ZMS}$ value without dose variations.

As can be seen from Table **1**, modes 23x2.12Gy and 4x10Gy have almost the same value of TCP (25.25% and 24.01%). Despite the almost identical result for TCP, it is evident that in the SBRT mode in all three cases of uncertainty in the dose per fraction [3 5 10]% - we have a greater uncertainty in TCP. Since 3% uncertainty in the SBRT technique is somewhat insufficient, in this type of treatment stricter criteria for dose uncertainty are required [ **82** , **83** , **84** ], so in these cases the impact of a 2% uncertainty on the TCP result is also considered. In this case, the result is $TCP_{mean}$ = 24.26 ± 5.35%, which is comparable in uncertainty to the case with 20x2.4Gy and 3% uncertainty. This is indicative of why in hypofractionation with high doses per fraction, stricter criteria are needed.

We will consider a case of irradiation in the Monday-Wednesday-Friday (extended) mode and compare it with the conventional - Monday-Friday. As the extended regimen analyzed by Alite et al. [ **41** ] and further investigated by Stavrev et al. [ **40** ] showed better tumor response to treatment, the impact of dose uncertainty on TCP will be addressed. The model parameters are chosen from the article [ **40** ], as $\lambda$ (repopulation) and the parameter accounting for the reoxygenation rate in the tumor, b, are arbitrarily chosen from the range in which they are considered there. The model parameters are: N = 3.1x10 $^{3}$ ,$\alpha_0 = 0.073Gy^{-1}$,$\beta_0 = 0.0013Gy^{-2}$, $\alpha_m = 0.108Gy^{-1}$, $\beta_m = 0.0028Gy^{-2}$, $d$ = 0.005d-$^{1}$, $d_f$ = 15Gy, $n_f$ = 5 and accordingly selected $\lambda$ = *0.05d $^{-1}$ [0 - 2]* and b =

*0.1d $^{-2}$ [0 - 0.15]*. The histogram of the distribution of TCP values at a dose uncertainty of 2% is shown in the following figure. The mode is Monday-Friday:

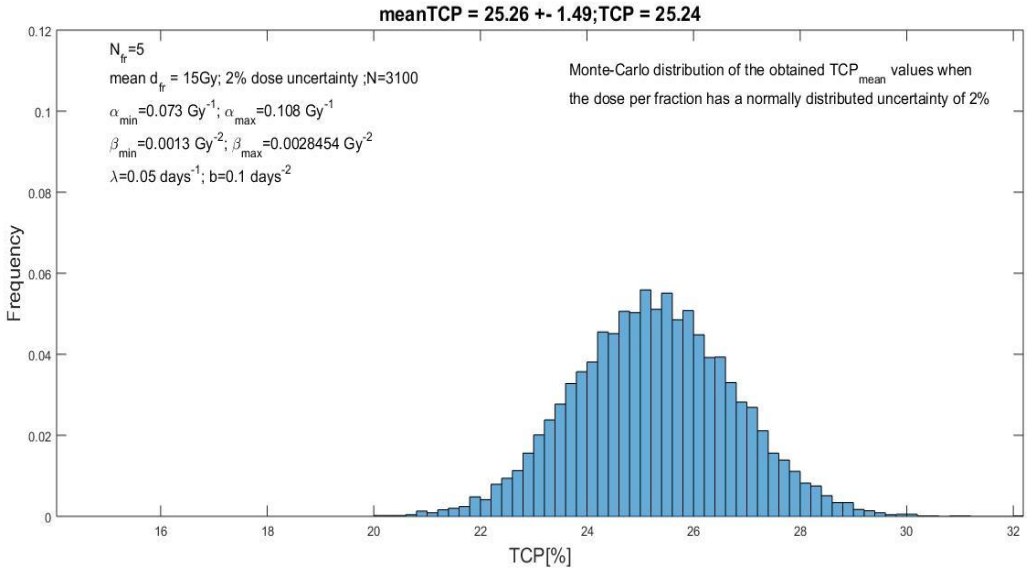


Figure 14 : Histogram of the distribution of TCP values as a function of frequency, at a dose uncertainty of 2%. Mode: from Monday to Friday. Fractionation: 5 x 15Gy

The minimum value of TCP is 20.05%, the maximum value is 32.19%, and the average value is 25.26 ±1.49%.

The following figure shows the Monday-Wednesday-Friday mode:

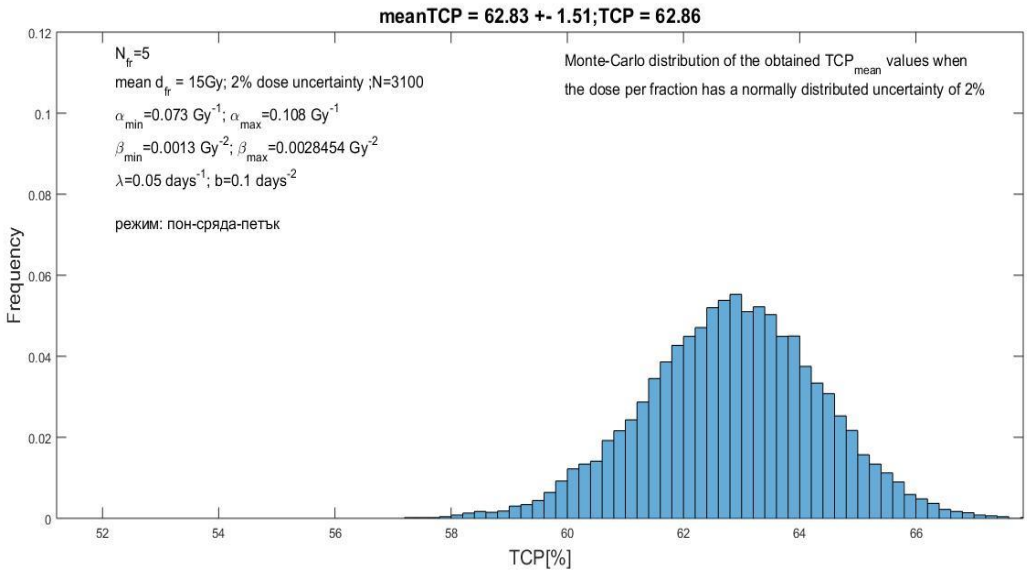


Figure 15 : Histogram of the distribution of TCP values as a function of frequency, at a dose uncertainty of 2%. Mode: Monday-Wednesday-Friday. Fractionation: 5x15Gy

TCP value is 57.21%, the maximum 67.85% , and the average value is 62.83±1.51% .

With 10% dose uncertainty, the results are as follows - for the Monday to Friday regime: $TCP_{mean}^{10\%\,(monday-friday)} = 25.94 \pm 8.76\%$, ($TCP_{min}$=3.83%, $TCP_{max}$=62.61%). For the Monday-Wednesday-Friday mode: $TCP_{mean}^{10\%\,(monday-wednesday-friday)} = 62.35 \pm 9.11\%$, ($TCP_{min}$=22.17%, $TCP_{max}$=88.33%).

In **conclusion**:

- Dose uncertainty plays significant role in the outcome of radiotherapy (in terms of TCP);
- Stronger impact of the dose uncertainty exists in SBRT radiation regimens (with high doses per fraction). That is why the criteria are stricter there as well.
- In all cases – the biggest deviations in TCP are found at TCP values in the range of 30%-70%. This follows logically from the fact that these TCP values are in the steepest part of the curve and small deviations in the dose change the TCP value the most.

# 7. Scientific contributions and publications related to the dissertation

The scientific and scientific-applied contributions of the present dissertation are:

- Data from the animal experiment of Fischer et al. were successfully fitted to the ZMS model accounting for cellular reoxygenation and thus the model was verified.
- TCP during hypofractionated radiotherapy was evaluated using two different TCP models – $TCP_{ZMS}$ and $TCP_{RN}$ .
- It was confirmed by the TCP models used that tumor control mainly depends on the death of the most radioresistant tumor cells in the cell conglomerate.
- The impact of dose uncertainty on the tumor control probability at different baseline values of this uncertainty was evaluated.

In the course of the research on this dissertation was written and published articles where the graduate is a co-author and one in which he is the first author. Posters were also presented at international conferences:

**Journal articles with an impact factor:**

1. Penev, D., Stavrev, P., Stavreva, N. , Pressyanov, D. Influence of dose uncertainty on TCP estimates: a model study. ***Eur. Phys. J. Spec. Top.*** 232, 1543–1547 (2023). https://doi.org/10.1140/epjs/s11734-023-00880-y ( **quartile Q2** ).

2. Stavrev PV, Stavreva N, Ruggieri R, Nahum AE, Tsonev P, Penev D, Pressyanov D. Theoretical investigation of the impact of different timing schemes in hypofractionated radiotherapy. ***Med . Phys.*** 2021 Jul;48(7):4085-4098. doi: 10.1002/mp.14908. Epub 2021 May 31. PMID: 33905547 ( **quartile Q1** ).

3. Stavrev P, Stavreva N, Penev D, Nahum A, Ruggieri R, Pressyanov D. Investigation of the effect of natural tumor cell death on radiotherapy outcomes. ***Phys. Med. Biol.*** 2018 Oct 9;63(20):205001. doi: 10.1088/1361-6560/aae05d. PMID: 30204124 ( **quartile Q1** ).

**Papers at international conferences, with extended abstracts published in journals with an impact factor:**

4. N. Stavreva, P. Stavrev, D. Penev, A. Nahum, R. Ruggieri, D. Pressyanov. On the possibility of estimating the radiosensitivity range in a cell mixture . April 2019, ***Radiotherapy and Oncology*** 133: S1029, DOI: 10.1016/S0167-8140(19)32314-X

5. P. Stavrev, N. Stavreva, R. Ruggieri, AE Nahum, D. Penev, A. Balabanova, D. Pressyanov. A user friendly Matlab code for TCP/NTCP estimation in HDR brachytherapy available. Dec 2021 ***Physica Medica*** 92: S184, DOI:10.1016/S1120-1797(22)00393-3

6. P. Stavrev, N. Stavreva, D. Penev, R. Ruggieri, AE Nahum, A. Balabanova, D. Georgiev, M. Gancheva, D. Pressyanov. Re-irradiation: Estimating NTCP when only the dDVHs for an OAR from the first and the second treatments are available, December 2021 ***Physica Medica*** 92: S183-S184, DOI: 10.1016/S1120-1797(22)00392-1

7. Stavreva, P. Stavrev, D. Penev Impact of natural tumor cell death on TCP N. ESTRO37 , April 2018, ***Radiotherapy and Oncology*** 127:S1081, DOI:10.1016/S0167-8140(18)322977

# 8. Literature


1. Ferlay J, Ervik M, Lam F, Colombet M, Mery L, Piñeros M, Znaor A, Soerjomataram I, Bray F (2020). Global Cancer Observatory: Cancer Today. Lyon, France: International Agency for Research on Cancer. Available from: https://gco.iarc.fr/today, accessed [07 02 2023]
2. RADIATION ONCOLOGY PHYSICS: A Handbook for Teachers and Students; EB Podgorsak – Technical Editor © the International Atomic Energy Agency, 2005
3. Fathy, MM, Hassan, BZ, El-Gebaly, RH et al. Dosimetric evaluation study of IMRT and VMAT techniques for prostate cancer based on different multileaf collimator designs. Radiat Environ Biophys 62, 97–106 (2023). https://doi.org/10.1007/s00411-022-01011-2
4. Liu H, Chang JY. Proton therapy in clinical practice. Chin J Cancer. 2011 May;30(5):315-26. doi: 10.5732/cjc.010.10529. PMID: 21527064; PMCID: PMC4013396
5. Thomas H, Timmermann B. Pediatric proton therapy. Br J Radiol. 2020 Mar;93(1107):20190601. doi: 10.1259/bjr.20190601. Epub 2019 Sep 19. PMID: 31529979; PMCID: PMC7066960
6. International Atomic Energy Agency. Absorbed dose determination in external beam radiotherapy, Technical Reports Series No. 398, IAEA, Vienna (2000)]
7. Gary A. Ezzell et al. - IMRT commissioning: Multiple institution planning and dosimetry comparisons, a report from AAPM Task Group 119, Med. Phys. 36 (11), November 2009, https://doi.org/10.1118/1.3238104
8. Eric E. Klein et al. Task Group 142 report: Quality assurance of medical accelerators, Medical Physics 36, 4197 (2009); doi: 10.1118/1.3190392
9. Daniel A. Low, Jean M. Moran, James F. Dempsey, Lei Dong, Mark Oldham - Dosimetry tools and techniques for IMRT, a report from AAPM Task Group 120, Medical Physics, Vol. 38, No. 3, March 2011, https://doi.org/10.1118/1.3514120
10. Hugo Palmans et al. Report No. TRS-483 - Dosimetry of small static fields used in external photon beam radiotherapy the IAEA-AAPM international Code of Practice for reference and relative dose determination (2018)
11. REGULATION No.2 OF FEBRUARY 5, 2018 ON THE CONDITIONS AND PROCEDURES FOR PROVIDING PROTECTION OF PERSONS FROM MEDICAL RADIATION, Effective from February 9, 2018. Issued by the Minister of Health
12. Pedro Andreo, David T. Burns, Alan E. Nahum, Jan Seuntjens, Frank Herbert Attix Fundamentals of Ionizing Radiation Dosimetry John Wiley & Sons, 2017, ISBN 3527409211,9783527409211
13. Alberts B, Johnson A, Lewis J, et al. Molecular Biology of the Cell. 4th edition. New York: Garland Science; 2002. Available from: https://www.ncbi.nlm.nih.gov/books/NBK21054/
14. Olive, Peggy L. "The Role of DNA Single- and Double-Strand Breaks in Cell Killing by Ionizing Radiation." Radiation Research, vol. 150, no. 5, 1998, pp. S42–51. JSTOR, https://doi.org/10.2307/3579807
15. Maier P, Hartmann L, Wenz F, Herskind C. Cellular Pathways in Response to Ionizing Radiation and Their Targetability for Tumor Radiosensitization. Int J Mol Sci. 2016 Jan 14;17(1):102. doi: 10.3390/ijms17010102. PMID: 26784176; PMCID: PMC4730344

16. Qian Li, Guoping Zhao, Wei Han, Shengmin Xu, Lijun Wu, Radiation target: Moving from theory to practice, Nuclear Analysis, Volume 1, Issue 2, 2022, 100024, ISSN 2773-1839, https://doi.org/10.1016/j.nucana.2022.100024
17. Caldecott, K. Single-strand break repair and genetic disease. Nat Rev Genet 9, 619–631 (2008). https://doi.org/10.1038/nrg2380
18. Biau J, Chautard E, Verrelle P, Dutreix M. Altering DNA Repair to Improve Radiation Therapy: Specific and Multiple Pathway Targeting. Front Oncol. 2019 Oct 10; 9:1009. doi: 10.3389/fonc.2019.01009. PMID: 31649878; PMCID: PMC6795692
19. N. Foray, CF Arlett, EP Malaise, Radiation-induced DNA double-strand breaks and the radiosensitivity of human cells: A closer look, Biochimie, Volume 79, Issues 9–10, 1997, Pages 567-575, ISSN 0300-9084 , https://doi.org/10.1016/S0300-9084(97)82005-6
20. Nickoloff JA, Sharma N, Taylor L. Clustered DNA Double-Strand Breaks: Biological Effects and Relevance to Cancer Radiotherapy. Genes (Basel). 2020 Jan 15;11(1):99. doi: 10.3390/genes11010099. PMID: 31952359; PMCID: PMC7017136
21. JF Ward The yield of DNA double-stand breaks produced intracellularly by ionizing radiation: a review, Int. J. Radiat. Biol. Vol. 57, No:6, 1141-1150, 1990
22. Toulany M. Targeting DNA Double-Strand Break Repair Pathways to Improve Radiotherapy Response. Genes (Basel). 2019 Jan 4;10(1):25. doi: 10.3390/genes10010025. PMID: 30621219; PMCID: PMC6356315
23. John B. Little - Cellular effects of ionizing radiation, The New England Journal of Medicine, 1968
24. Wanyeon Kim, Sungmin Lee, Danbi Seo, Dain Kim, Kyeongmin Kim, EunGi Kim, JiHoon Kang, Ki Moon Seong HyeSook Youn and BuHyun Youn, Cellular Stress Responses in Radiotherapy, Cells. 2019 Sep; 8(9): 1105. Doi: 10.3390/cells8091105
25. Puck, TT & Marius, PI - Action of x-rays on mammalian cells (1956) J. exp. Med. 103: 653
26. HEWITT HB, WILSON CW. A survival curve for mammalian cells irradiated in vivo. Nature. 1959 Apr 11;183(4667):1060-1. doi: 10.1038/1831060a0. PMID: 13644286
27. Dr. DE Lea - Actions of Radiations on Living Cells, Cambridge: At the University Press, 1946
28. Kellerer, AM, and Rossi, H D. THEORY OF DUAL RADIATION ACTION. United States: N. p., 1972. Web
29. Chadwick, KH & Leenhouts, HP A molecular theory of cell survival. Phys Med Biol (1973), 18, 78
30. Lea, DE, Catcheside, DG The mechanism of the induction by radiation of chromosome aberrations in Tradescantia. Journ. of Genetics 44, 216–245 (1942). https://doi.org/10.1007/BF02982830
31. Hubenak JR, Zhang Q, Branch CD, Kronowitz SJ. Mechanisms of injury to normal tissue after radiotherapy: a review. Plast Reconstr Surg. 2014 Jan;133(1):49e-56e. doi: 10.1097/01.prs.0000440818.23647.0b. PMID: 24374687; PMCID: PMC3921068
32. DS Chang et al., Basic Radiotherapy Physics and Biology, Springler Science (2014) DOI 10.1007/978-3-319-06841-1_22
33. H. Rodney Withers. Treatment-Induced Accelerated Human Tumor Growth, Seminars in Radiation Oncology, Vol 3, No 2 (April), 1993: pp 135-143, DOI: https://doi.org/10.1016/S1053-4296(05)80089-X
34. Campillo N, Falcones B, Otero J, Colina R, Gozal D, Navajas D, Farré R, Almendros I. Differential Oxygenation in Tumor Microenvironment Modulates Macrophage and Cancer Cell Crosstalk:

Novel Experimental Setting and Proof of Concept. Front Oncol. 2019 Feb 6;9:43. doi: 10.3389/fonc.2019.00043. PMID: 30788287; PMCID: PMC6373430

35. Khan, B., Nhan, TNT, Chau, HNM, & Nhi, NTY Roles of hypoxia in tumor progression and novel strategies for cancer treatment. Biomedical Research and Therapy, 2022, 9(10), 5361-5374. https://doi.org/10.15419/bmrat.v9i10.774
36. Stavreva N, Warkentin B, Stavrev P, Fallone BG. Investigating the effect of clonogen resensitization on the tumor response to fractionated external radiotherapy. Med Phys 2005; 32:720e5
37. J. Denekamp and A. Dasu, "Inducible repair and the two forms of tumor hypoxia—time for a paradigm shift," Acta Oncol. 38, 903–918 s1999d
38. A. Dasu, I. Toma-Dasu, and M. Karlsson, "Theoretical simulation of tumor oxygenation and results from acute and chronic hypoxia," Phys. Med. Biol. 48, 2829–2842 s2003d
39. Ruggieri, R.; Stavreva, N.; Naccarato, S.; Stavrev, P. Applying a hypoxia-incorporating TCP model to experimental data on rat sarcoma. Int. J. Radiat. Oncol. Biol. Phys. 2012, 83, 1603–1608
40. Stavrev PV, Stavreva N, Ruggieri R, Nahum AE, Tsonev P, Penev D, Pressyanov D. Theoretical investigation of the impact of different timing schemes in hypofractionated radiotherapy. Med Phys. 2021 Jul;48(7):4085-4098. doi: 10.1002/mp.14908. Epub 2021 May 31. PMID: 33905547
41. Alite F, Stang K, Balasubramanian N, et al. Local control dependence on consecutive vs. nonconsecutive fractionation in lung stereotactic body radiation therapy. Radiother Oncol. 2016; 121:9–14
42. Withers HR. Cell cycle redistribution as a factor in multifraction irradiation. Radiology. 1975a;114(1):199–202
43. Syljuåsen, RG Cell Cycle Effects in Radiation Oncology. In: Wenz, F. (eds) Radiation Oncology. Springer, Cham. (2019). https://doi.org/10.1007/978-3-319-52619-5_101-1
44. Terasima T, Tolmach LJ: Variations in several responses of HeLa cells to x-irradiation during the division cycle. BiophysJ 3:11-33, Jan 1963
45. Elkind MM: Sublethal x-ray damage and its repair in mammalian cells. [In] Radiation Research, Silini G, ed. Amsterdam, North Holland Pub Co, 1967, pp 558-586
46. Mauro F, Madoc-jones H: Age-response to x-radiation of murine lymphoma cells synchronized in vivo. Proc Nat Acad Sci 63:686-691, Jul 1969
47. Hellman S: X-irradiation of the hematopoietic stem cell compartment. Frontiers of Radiation Therapy and Oncology 6:415-427, 1972
48. HR Withers, KA Mason: The kinetics of recovery in irradiated colonic mucosa of the mouse Cancer. 1974 Sep;34(3): suppl:896-903
49. Ryan K. Funk, MD*, Abigail L. Stockham, MD, Nadia N. Issa Laack, MD, MS - Basics of Radiation Therapy 2016 https://doi.org/10.1016/B978-0-323-44227-5.00003- X
50. Biau J., Chautard E., Verrelle P., Dutreix M. Altering DNA repair to improve radiation therapy: Specific and multiple pathway targeting. Front. Oncol. 2019; 9:1009. doi: 10.3389/fonc.2019.01009
51. Lt Gen SR Mehta, AVSM, VSM, PHS*, Maj V Suhag+, M Semwal#, Maj N Sharma* Radiotherapy: Basic Concepts and Recent Advances, MJAFI, Vol. 66, No. 2, 2010
52. Nima Ghaderi,1,† Joseph Jung,1,† Sarah C. Brüningk,2,3 Ajay Subramanian,4 Lauren Nassour,5 and Jeffrey Peacock5,* A Century of Fractionated Radiotherapy: How Mathematical Oncology Can Break the Rules, Int J Mol Sci. 2022 Feb; 23(3): 1316. 10.3390/ijms23031316

53. Munro TR and Gilbert CW 1961 The relationship between tumor lethal doses and the radiosensitivity of tumor cells Br. J. Radiol. 34 246–51
54. EH PORTER, The statistics of dose/cure relationships for irradiated tumors. Part **II** . Bro. J. Radiol. 53, 336-345 (1980)
55. HD SUIT, RJ SHALEK, and R. WETTE, Radiation response of C3H mammary carcinoma. In Cellular Radiation Biology, pp. 514-530. Williams & Wilkins, Baltimore, 1965
56. Zaider M and Minerbo GN 2000 Tumor control probability: a formulation applicable to any temporal protocol of dose delivery Phys. Med. Biol. 45 279–93
57. Fischer JJ. Theoretical considerations in the optimization of dose distribution in radiation therapy. Br J Radiol 1969; 42:925–30
58. Pavel Stavrev, Colleen Schinkel, Nadia Stavreva, Brad Warkentin, Marco Carlone & B. Gino Fallone (2010) Population TCP estimators in case of heterogeneous irradiation: A new discussion of an old problem, Acta Oncologica, 49:8, 1293-1303, DOI: 10.3109/02841861003649232
59. Brenner DJ. Dose, volume, and tumor-control predictions in radiotherapy. Int J Radiat Oncol Biol Phys 1993; 26:171–9
60. Webb S. Optimum parameters in a model for tumor-control probability including interpatient heterogeneity. Phys Med Biol 1994; 39:1895–914
61. Carlone M, Warkentin B, Stavrev P, Fallone B. Fundamental form of a population TCP model in the limit of large heterogeneity. Med Phys 2006; 33:1634–42
62. van Putten LM. Tumor reoxygenation during fractionated radiotherapy; studies with a transplantable mouse osteosarcoma. Eur J Cancer. 1968; 4:172–182
63. Fischer J J and Moulder JE 1975 The steepness of the dose-response curve in radiation therapy. Theoretical considerations and experimental results Radiology 117 179–84
64. Fowler JF, Denekamp J, Sheldon PW, et al. Optimum fractionation in X-ray treatment of C3H mouse mammary tumors. Br J Radiol. 1974; 47:781–789
65. Tarnawski R, Widel M and Skladowski K 2003 Tumor cell repopulation during conventional and accelerated radiotherapy in the in vitro megacolony culture Int. J. Radiat. Oncol. Biol. Phys. 55 1074–81
66. Stavrev P, Stavreva N, Penev DN, Nahum AE, Ruggieri R, Pressyanov DS. Investigation of the effect of natural tumor cell death on radiotherapy outcomes. Phys Med Biol. 2018; 63:205001
67. Kendall DG 1948 On the generalized 'birth and death' process Ann. Stat. Math. 19 1–15
68. NAStavreva, PVStavrev, B. Warkentin and BGFallone- Investigating the effect of cell repopulation on the tumor response to fractionated external radiotherapy, Med. Phys. 30(5), May 2003
69. Wenzl, T., Wilkens, JJ Theoretical analysis of the dose dependence of the oxygen enhancement ratio and its relevance for clinical applications. Radiat Oncol 6, 171 (2011). https://doi.org/10.1186/1748-717X-6-171
70. Jackson A, Ten Haken RK, Robertson JM, Kessler ML, Kutcher GJ and Lawrence TS 1995 Analysis of clinical complication data for radiation hepatitis using a parallel architecture model Int. J. Radiat. Oncol. Biol. Phys. 31 883–91
71. Stavrev P, Niemierko A, Stavreva N and Goitein M 2001 The application of biological models to clinical data Phys. Med. 17 71–82
72. Porter EH. The statistics of dose/cure relationships for irradiated tumors. Part **I.** _ Br J Radiol. 1980; 53:210–227

73. Stavrev P, Stavreva N, Ruggieri R, Nahum AE. On differences in radiosensitivity estimation: TCP experiments versus survival curves. A theoretical study. Phys Med Biol. 2015; 60: N293–N299
74. Stavreva N, Nahum A, Markov K, Ruggieri R, Stavrev P. Analytical investigation of the possibility of parameter invariant TCP-based radiation therapy plan ranking. Acta Oncol. 2010;49(8):1324–1333
75. Chapman JD. Can the two mechanisms of tumor cell killing by radiation be exploited for therapeutic gain? J Radiat Res 2013; 55:2e9. http://dx.doi.org/10.1093/jrr/rrt111
76. Nahum AE. The radiobiology of hypofractionation. Clin Oncol. 2015;27(5):260–269
77. Ruggieri R. Hypofractionation in non-small cell lung cancer (NSCLC): suggestions from modeling both acute and chronic hypoxia. Phys Med Biol. 2004; 49:4811–4823
78. Ruggieri R, Nahum AE. The impact of hypofractionation on simultaneous dose-boosting to hypoxic tumor subvolumes. Med Phys. 2006; 33:4044–4055
79. D. Thwaites, J. Phys Conf. Ser. 444, 012006 (2013) DOI 10.1088/1742-6596/444/1/012006
80. Dimitar Penev, Pavel Stavrev, Nadejda Stavreva, and Dobromir Pressyanov Influence of dose uncertainty on TCP estimates: a model study 2023 Eur. Phys. J. Spec. Top. https://doi.org/10.1140/epjs/s11734-023-00880-y
81. Stavrev P. et al., The impact of different timing schedules on prostate HDR-mono-brachytherapy. A TCP modeling investigation. Cancers 13(19), 4899 (2021)
82. Zhen H, Nelms BE, Tome WA. Moving from gamma passing rates to patient DVH-based QA metrics in pretreatment dose QA. Med Phys. 2011 Oct;38(10):5477-89. doi: 10.1118/1.3633904. PMID: 21992366
83. Heilemann G, Poppe B, Laub W. On the sensitivity of common gamma-index evaluation methods to MLC misalignments in Rapidarc quality assurance. Med Phys. 2013 Mar;40(3):031702. doi: 10.1118/1.4789580. PMID: 23464297
84. Fredh A, Scherman JB, Fog LS, Munck af Rosenschöld P. Patient QA systems for rotational radiation therapy: a comparative experimental study with intentional errors. Med Phys. 2013 Mar;40(3):031716. doi: 10.1118/1.4788645. PMID: 23464311

# *Acknowledgments*

I express my gratitude to all the teachers with whom life met me during my studies.

I express special thanks to Prof. Dobromir Presiyanov, who believed in me and who was always there for me with guidance and ideas related to the writing of this dissertation work.

I express special thanks to Dr. Pavel Stavrev and Dr. Nadezhda Stavreva, who inspired me to continue my scientific development after the master's degree. Dr. Stavrev is the person who opened the world of radiobiological modeling to me. He made me look at medical physics from another angle unknown to me before. He has been by my side all these years, helping and inspiring.

I want to thank my parents who made me the person I am and always give me the right advice. I love you!

And last but not least, I want to thank my wife Victoria! The person who was there for me in my highs and lows. The person who helped me when I lost motivation and gave me the drive to keep learning and developing! Thank you for putting up with the days when I was studying and didn't have enough time for you. Thank you for accepting my cause to write this work as your own. Thank you for gifting me with our beautiful daughter Anna! Our sun, our smile, our love!